

The Impact of Exogenous Mitochondrial Transfer on Skeletal Muscle Injury in Mice



by

Fazal Wahid

Department of Biochemistry,

Quaid-i-Azam University

Islamabad, Pakistan

2023

The Impact of Exogenous Mitochondrial Transfer on Skeletal Muscle Injury in Mice



A thesis submitted in partial fulfillment of the requirements for the

Degree of Master of Philosophy

in

Biochemistry/Molecular Biology

by

Fazal Wahid

Department of Biochemistry,

Quaid-i-Azam University Islamabad, Pakistan

2023

Quaid-i-Azam University, Islamabad, PAKISTAN
Department of Biochemistry
Faculty of Biological Sciences

CERTIFICATE

This thesis, submitted by **Mr. Fazal Wahid** to the Department of Biochemistry, Faculty of Biological Sciences, Quaid-i-Azam University, Islamabad, Pakistan, is accepted in its present form as satisfying the thesis requirement for the Degree of Master of Philosophy in Biochemistry/Molecular Biology.


Examination Committee:

1. **External Examiner:**
Dr. Muhammad Jadoon Khan

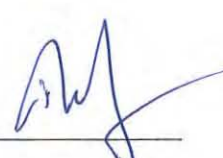
Associate Professor
Department of Biosciences
COMSATS University Islamabad

Signature: 

2. **Supervisor:**
Dr. Muhammad Rizwan Alam

Signature: 

3. **Chairperson:**
Prof. Dr. Iram Murtaza

Signature: 

Dated:

October 31, 2023

DECLARATION

I, **Fazal Wahid**, hereby declare that any part of this dissertation is not plagiarized, and all work was carried out in accordance with regulation set by the Quaid-i-Azam University. No part of this thesis has been previously presented for any other degree. If found anything contrary, I shall be held responsible.

Fazal Wahid

Dedicated

to

My beloved parents and siblings

whom unwavering support, love, sacrifices

and prayers are the guiding light

in my journey of success

ACKNOWLEDGEMENTS

Above all, I humbly acknowledge the abundant blessings and guidance from the Divine, Allah, the almighty that have played integral role in the successful completion of my research.

I am very thankful to the Chairperson Department of Biochemistry **Dr. Iram Murtaza** for providing us with a healthy research environment.

It is my pleasure to express deep and sincere gratitude to my mentor and guide, **Dr. M Rizwan Alam**, for giving me the opportunity to do research and providing invaluable guidance throughout this research. His dynamism, vision, sincerity and persistent motivation have deeply inspired me. His scholarly advice, meticulous scrutiny and scientific approach have helped me to a great extent to accomplish this task. He has taught me the way to present the research work as clearly as possible. It was a great privilege and honor to work and study under his guidance. I am extremely grateful for what he has offered me.

I am also very thankful to all my lab colleagues **Durre Shehwar, Rabia Shireen, Sehrish Gohar Ali, Shafia Khan, Amna Falak, Hina Shahid Laiba Abbasi, Faseeha Azmat, Ameer Hamza, Khadeeja Ahsan and Ajwa Ishfaq** who consistently inspire excellence and foster a collaborative and innovative spirit. Their togetherness has made this golden period memorable and life lesson. I owe my thanks to my PhD senior **Saima Barki** who supported me not only in my lab work but always provided a comfortable environment. I am highly thankful to staff of the Department of Biochemistry for their support and guidance.

I am extremely grateful to my parents and siblings for their love, sincerity, prayers, care and sacrifices for where I stand now. In particular I extend my gratitude to **Fati Ullah** and **Sher Aziz** for their persistent backing and upliftment.

Table of Contents

| | | |
|----------------|--|------------|
| i | List of figures ----- | i |
| ii | List of abbreviations----- | iii |
| iii | Abstract ----- | vi |
| 1 | Introduction ----- | 1 |
| 1.1 | Skeletal Muscles ----- | 1 |
| 1.1.1 | Muscle fibers are the cells of skeletal muscles ----- | 1 |
| 1.1.2 | Molecular mechanism of skeletal muscle contraction and relaxation ----- | 2 |
| 1.2 | Types of skeletal muscles fibers ----- | 3 |
| 1.2.1 | The fast and slow contracting fibers depend on speed of their energy metabolism and ATPase activity----- | 3 |
| 1.3 | Skeletal muscle injuries ----- | 4 |
| 1.3.1 | Contraction-induced injury ----- | 4 |
| 1.3.2 | Volumetric muscle loss injury ----- | 4 |
| 1.3.3 | Skeletal muscle burn injury----- | 5 |
| 1.3.4 | Biotoxin-induced skeletal muscle injury ----- | 5 |
| 1.3.5 | Ischemia reperfusion injury ----- | 5 |
| 1.3.6 | Skeletal muscle atrophy----- | 6 |
| 1.3.6.1 | Molecular mechanisms of skeletal muscle atrophy ----- | 7 |
| 1.3.6.2 | Upstream signaling pathways of skeletal muscle atrophy ----- | 7 |
| 1.3.6.3 | Calpains and caspases ----- | 7 |
| 1.3.6.4 | Ubiquitin-proteome system ----- | 8 |
| 1.3.6.5 | Autophagy-lysosome system ----- | 9 |
| 1.3.7 | BaCl ₂ -induced skeletal muscle injury ----- | 12 |
| 1.4 | Mitochondrial dysfunction in skeletal muscle injuries ----- | 13 |
| 1.4.1 | Ca ²⁺ overload ----- | 13 |
| 1.4.2 | Oxidative stress ----- | 14 |
| 1.4.3 | Mitochondrial dynamics ----- | 15 |
| 1.4.4 | Mitophagy ----- | 16 |
| 1.5 | Therapeutic strategies to repair skeletal muscle injuries ----- | 16 |
| 1.5.1 | Natural products as therapeutics ----- | 16 |
| 1.5.2 | Other therapies ----- | 17 |
| 1.6 | Mitochondrial transplantation therapy ----- | 18 |

| | | |
|-------|--|----|
| 1.6.1 | In vitro mitochondrial transplantation ----- | 18 |
| 1.6.2 | In vivo mitochondrial transplantation ----- | 20 |
| 1.7 | Exogenous mitochondrial sources for in vivo MT ----- | 20 |
| 1.8 | MT in skeletal muscles injuries ----- | 21 |
| 2 | Materials and methods ----- | 24 |
| 2.1 | Ethical approval of the study and animal handling ----- | 24 |
| 2.2 | Mitochondrial isolation ----- | 24 |
| 2.3 | Enrichment of mitochondrial crude extract via Differential centrifugation ----- | 24 |
| 2.4 | Mitochondrial protein quantification ----- | 25 |
| 2.5 | Mitochondrial oxygen consumption rate ----- | 26 |
| 2.6 | MTT assay ----- | 27 |
| 2.7 | Mitochondrial transplantation (MT) ----- | 28 |
| 2.8 | Establishment of skeletal muscle injury models ----- | 28 |
| 2.9 | Dexamethasone-induced muscle atrophy mice model ----- | 28 |
| 2.10 | Barium chloride (BaCl ₂)-induced skeletal muscle injury mice model ----- | 29 |
| 2.11 | TTC staining assay ----- | 30 |
| 2.12 | Lactate dehydrogenase (LDH) assay ----- | 31 |
| 2.13 | Histological analysis ----- | 32 |
| 2.14 | Statistical analysis ----- | 32 |
| 3 | Results ----- | 33 |
| 3.1 | High dose of dexamethasone (20mg/kg) induce severe physical impairment ----- | 33 |
| 3.1.1 | Dexamethasone (20mg/kg) reduced mice body weight ----- | 33 |
| 3.1.2 | High dose of dexamethasone caused a reduction in individual muscles weight ----- | 36 |
| 3.1.3 | Dexamethasone (20mg/kg) reduces muscle fiber cross sectional area (CSA) ----- | 36 |
| 3.1.4 | Dexamethasone upraised serum LDH level ----- | 36 |
| 3.2 | Low dose of dexamethasone (5mg/kg) induced muscle atrophy ----- | 40 |
| 3.3 | Comparative effects of low (5mg/kg) and high dose (20mg/kg) dexamethasone On body weight and serum LDH levels ----- | 43 |
| 3.4 | BaCl ₂ -induced skeletal muscle injury ----- | 46 |
| 3.4.1 | BaCl ₂ - induced muscle necrosis ----- | 46 |
| 3.4.2 | MT and muscles mass in dexamethasone-treated mice ----- | 46 |
| 3.5 | Isolated mitochondria demonstrated respiration competency and viability --- | 50 |

| | | |
|-------------|--|----|
| 3.6 | Mitochondrial transfer (MT) recovered the body weight loss in dexamethasone-treated mice ----- | 52 |
| 3.7 | MT and muscle mass in Dexamethasone-treated Mice ----- | 52 |
| 3.8 | Impact of MT on Muscle Volume ----- | 55 |
| 3.9 | MT affected serum LDH level ----- | 54 |
| 3.10 | MT demonstrated positive effect on muscle weight gain ----- | 58 |
| 3.11 | MT exhibited no change in serum LDH level ----- | 58 |
| 4 | Discussion ----- | 61 |
| 5 | References ----- | 65 |

List of Figures

| Sr. No. | Title of Figures | Pg. No. |
|---------|---|---------|
| 1.1 | Schematic diagram of skeletal muscle organization from muscle to myofibril | 2 |
| 1.2 | Ubiquitin-proteasome pathway of skeletal muscle atrophy | 9 |
| 1.3 | The formation of autophagosome via autophagy lysosome system in skeletal muscle atrophy | 11 |
| 1.4 | Mitochondrial stress due to elevated ROS and Ca ²⁺ | 14 |
| 1.5 | Skeletal muscle injuries and mitochondrial stress by elevated ROS and Ca ²⁺ | 15 |
| 1.6 | Mitochondrial transfer to an injured skeletal muscle | 21 |
| 2.1 | Schematic diagram of mitochondrial isolation from healthy mice liver tissues | 25 |
| 2.2 | Standard curve for BSA | 26 |
| 2.3 | Experimental plan for dexamethasone-induced skeletal muscle atrophy model generation | 29 |
| 2.4 | Experimental design of BaCl ₂ -induced muscle injury model | 30 |
| 2.5 | TTC staining and observation under stereomicroscope | 31 |
| 3.1 | The physical features of mice with dexamethasone high dose (20mg/kg) | 34 |
| 3.2 | Loss of body weight in mice administered with high dose of dexamethasone | 35 |
| 3.3 | Change in muscle mass of dexamethasone-treated mice | 37 |
| 3.4 | Reduced muscle fiber cross-section area in dexamethasone treated mice | 38 |
| 3.5 | The observable increase in serum LDH level in dexamethasone-treated mice | 39 |
| 3.6 | Low dose of dexamethasone caused reduction in body weight | 41 |
| 3.7 | Change in muscle mass due to low dose of dexamethasone | 42 |
| 3.8 | Low dose of dexamethasone caused a reduction in serum LDH release | 43 |
| 3.9 | Dexamethasone high and low doses have differentially reduced body weight and serum LDH levels | 45 |
| 3.10 | BaCl ₂ induced muscle injury in hind-limb muscles | 47 |
| 3.11 | BaCl ₂ -induced necrosis in GS muscle | 48 |
| 3.12 | Increased serum LDH level in BaCl ₂ treated mice | 49 |
| 3.13 | Functional assessment of isolated mitochondria | 51 |
| 3.14 | Mitochondrial transplantation alleviated body weight loss | 53 |
| 3.15 | MT resulted in no change in individual muscle weight in dexamethasone-treated mice | 54 |
| 3.16 | Mitochondrial transplantation and muscle volume | 56 |

| | | |
|------|--|----|
| 3.17 | Serum LDH release was decreased upon MT | 57 |
| 3.18 | MT demonstrated increased trend in muscle mass of BaCl ₂ treated mice | 59 |
| 3.19 | MT revealed no impact on LDH level | 60 |

List of abbreviations

| | |
|-------------------|---|
| $\Delta\Psi_m$ | Mitochondrial membrane potential |
| AAR | Area at risk |
| Akt | Proteins Kinase B |
| AMPK | AMP-activated protein kinase |
| Atgs | Autophagy-related genes |
| Atrogin-1 | Atrophy gene-1 |
| BaCl ₂ | Barium Chloride |
| BLAST | Biophotonic-laser-assisted surgery tool |
| Bnip3 | BCL2 Interacting Protein 3 |
| BSA | Serum Albumin |
| CAP | Chloramphenicol |
| Ca ²⁺ | Calcium |
| CK | Creatine kinase |
| CSA | Cross sectional area |
| CTX | Cardiotoxin |
| Dexa | Dexamethasone |
| EDTA | Ethylenediaminetetraacetic Acid |
| ELAM | Elamipritice |
| EF | Efrapeptin |
| ERK | Extracellular Signal-Regulated Kinase |
| EVs | Extra cellular vesicles |
| FoxO3 | Forkhead Box O3 |
| GABARAP | Gamma-aminobutyric acid receptor-associated protein |
| GS | Gastrocnemius |
| H/E | Haematoxylin and eosin |
| HB | Homogenization buffer |
| HDAC | Histone Deacetylase |
| HEPES | 4-(2-Hydroxyethyl)piperazine-1-ethanesulfonic acid) |
| IL-6 | Interleukin-6 |
| IP | Interperitonium |
| IRI | Ischemia reperfusion injury |

| | |
|----------------------------------|---|
| JAK-STAT3 | Janus kinase-Signal Transducer and Activator of Transcription 3 |
| KCl | Potassium Chloride |
| KH ₂ PO ₄ | Potassium Dihydrogen Phosphate |
| LC3 | Microtubule-associated protein 1A/1B-light chain 3 |
| LDH | Lactate dehydrogenase |
| MFN1/2 | Mitofusin or Mitochondrial fusion protein |
| mNSC | Motor neurons |
| mPTP | Mitochondrial Permeability transition pore |
| MSCs | Mesenchymal stem cells |
| MT | Mitochondrial transplantation |
| mtDNA | Mitochondrial DNA |
| mTOR | Mechanistic Target of Rapamycin |
| MuRF1 | Muscle RING Finger 1 |
| N2a | Neuroblastoma |
| Na ₂ HPO ₄ | Disodium Hydrogen Phosphate |
| NaCl | Sodium Chloride |
| NAD | Nicotinamide Adenine Dinucleotide |
| NF- κ B | Nuclear Factor-kappa B |
| NR | Necrotic region |
| OMM | Outer Mitochondrial Membrane |
| OXPHOS | Oxidative phosphorylation |
| PBS | Phosphate-Buffer Saline |
| PC-12 | Pheochromocytoma cell |
| Pep-1 | Penetrating peptide |
| PGC-1 α | Peroxisome Proliferator-Activated Receptor Gamma |
| PI3K/Akt | Phosphoinositide 3-kinase |
| PIPs | Phosphatidylinositol Phosphates |
| PMSF | Phenylmethylsulfonyl fluoride |
| QD | Quadriceps |
| ROS | Reactive oxygen species |
| TA | Tibialis anterior |
| TNF- α | Tumor necrosis factor alpha |
| TRIM32 | Tripartite Motif Containing 32 |

| | |
|---------|---|
| TTC | 2,3,5-triphenyltetrazolium chloride |
| UC-MSCs | Umbilical cord mesenchymal stem cells |
| ULK1 | Unc-51 Like Autophagy Activating Kinase 1 |
| UPS | Ubiquitin-proteasome system |
| VC | Vehicle control |
| VML | Volumetric muscle loss |

Abstract

Musculoskeletal disorders are a global health burden that end up in amputation and lifelong dependency. Skeletal muscle injuries may be either pathological such as traumatic, myotoxic or physiological such as skeletal muscle atrophy. Muscle injuries are known to impair mitochondrial health, creating energy deficit, reduced muscle regeneration and activation of cell death pathways. Mitochondrial transplantation therapy has emerged as a novel promising therapeutic strategy to alleviate impacts of mitochondrial dysfunction in skeletal muscle injuries. This study was designed to assess the therapeutic impact of crude mitochondrial preparations from healthy mouse livers on the skeletal muscle atrophy and injuries in rodent models. To this end BALB/c albino mice were used to develop two different models of skeletal muscle injuries including muscle atrophy using dexamethasone (dexa) and myotoxic injury with barium chloride (BaCl₂). Muscle injury models were evaluated by measuring changes in body and muscle weight, serum lactate dehydrogenase (LDH), limb muscle fiber cross-sectional area (CSA) and cell death through infarct size measurement using TTC staining. Mitochondria isolated from healthy mice liver through differential centrifugation method were functionally assessed using oxygen consumption rate and MTT assay prior to their use as therapeutic tool against muscle injuries. Dexa-treated mice showed a significant reduction in body weight, and muscle fiber cross sectional area. Likewise, a decreasing trend in muscle mass and size was observed as compared to vehicle control (VC). Similarly, dexa treatment resulted in increased serum LDH release compared to VC. BaCl₂-treated mice also showed a non-significant decrease in muscle weight with an increase in necrotic area and serum LDH levels. Mitochondrial transplantation insignificantly increased muscle mass while lowered serum LDH level in dexa-treated mice undergoing muscle atrophy. Likewise mitochondrial transfer also insignificantly increased the weight of muscles in the BaCl₂ group compared to control. Thus, our results confirm that mitochondrial transplantation can be used as a promising therapeutic strategy against muscle atrophy and myotoxic muscle injuries.

Key word: Skeletal muscle injury, mitochondrial transplantation, muscle atrophy, dexamethasone, Barium Chloride (BaCl_2), Lactate dehydrogenase (LDH)

1. Introduction

1.1 Skeletal muscles

Skeletal muscles are one of the major organs of musculoskeletal system of the body that comprises almost 40% of total body weight. The other types of muscles are cardiac and smooth muscles. Skeletal muscles act as the chief energy metabolism hub. It is one of the major reservoir of proteins which homes 50-70% of total body proteins, whereby approximately 30-50% protein turnover occurs (Evans, 2010). Besides proteins, it also stores other nutrients such as carbohydrates, amino acids, and lipids. The role that skeletal muscle plays in the body can be categorized into two domains (Dave *et al.* , 2021; Lin Yin *et al.* , 2021). From the mechanical perspective, it provides energy by consuming the chemical energy present in molecules to yield power, strength, maintain and change body postures and useful movements that help individuals to survive independently. While from the metabolic viewpoint, skeletal muscle stores substrates like amino acids and carbohydrates to produce heat form the combustion reactions to maintain core body temperature. Similarly, it releases stored nutrient in blood circulation to recover blood-sugar levels (Frontera *et al.* , 2015; Liang *et al.* , 2020a).

Each skeletal muscle is composed of thousands of cells called muscle fiber that are bundled together by a sheet of connective tissue (**Fig.1.1**). The outer sheath that surrounds the whole muscle is known as epimysium (Gao *et al.* , 2008). Muscles cells groups, also called fasciculi, are further wrapped by another sheath called perimysium (Gao *et al.*, 2008), while the innermost connective tissue membrane covering each muscle fiber is known as endomysium. Furthermore, each muscle fiber contain many myofibrils which are the main structures involved in muscle function (Frontera *et al.*, 2015).

1.1.1 Muscle fibers are the cells of skeletal muscles

The cell of a skeletal muscle called muscle fiber is an elongated, cylinder-shaped structure that extends through the entire length of a muscle (Fortin *et al.* , 2014). A single muscle fiber is composed of parallelly placed, elongated and cylindrical bundles of a large number of myofibrils. Myofibril is the core contractile structure of a muscle cell. It is composed of regular patterns of cytoskeletal

elements, the thick and thin filaments, which are highly organized and fashioned in a way to produce tension and muscle contraction, (**Fig. 1.1**) (Frontera *et al.*, 2015; Raven *et al.*, 2012)

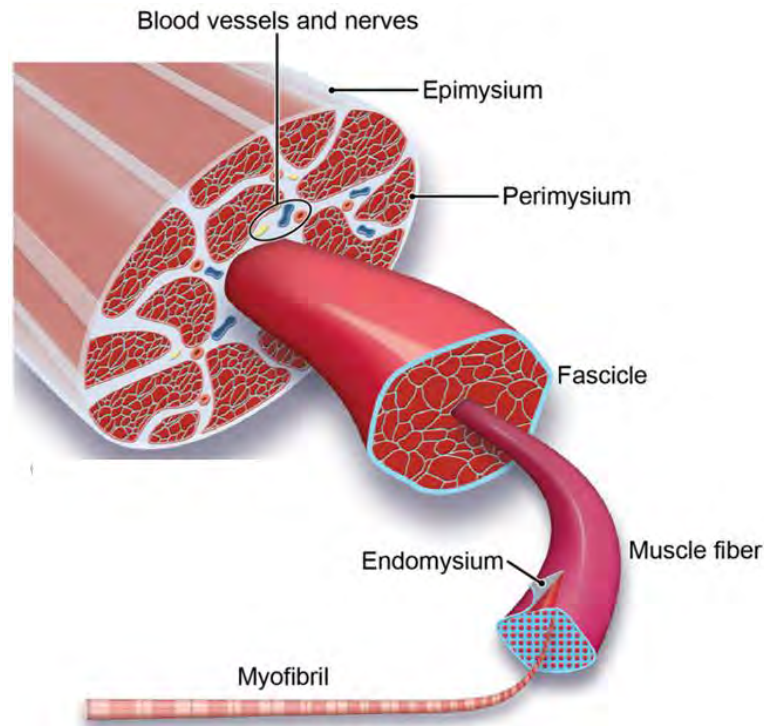


Fig. 1.1 Schematic diagram of skeletal muscle organization from muscle to myofibril (Jennings *et al.*, 2017).

1.1.2 Molecular mechanism of skeletal muscle contraction and relaxation

Muscle contraction can be defined as the shortening of the sarcomere as a result of sliding movement of thin filaments over thick ones (Pham *et al.*, 2020). Sarcomere do not shorten in reality; rather thin filaments slide over thick filaments towards its centre and is known as sliding filament mechanism, or muscles contraction. Electrical signal from the brain innervates muscle cells and cause Ca^{2+} release from endoplasmic reticulum. Ca^{2+} binds with a protein complex called troponin-tropomyosin complex causing it to move away from binding site of thick and thin filaments that is necessary for muscle contraction (Pham *et al.*, 2020). During the relaxation process, cytosolic Ca^{2+} is taken back into the lateral sacs by energy consuming channels, Ca^{2+} -ATPase pumps, causing troponin-tropomyosin complex to again mask binding sites of thin and

thick filaments (McCuller *et al.* , 2022). This allows the sliding back of thin filaments to their resting position and as a result ends up into the relaxation of whole muscle (Hopkins, 2006; Kuo *et al.* , 2015; Phung *et al.* , 2020). Moreover, there are distinct types of skeletal muscle fibers which are responsible for their varying function regarding strength and speed of contraction others (J. A. Smith *et al.* , 2023).

1.2 Types of skeletal muscles fibers

A human body has about 600 skeletal muscles in his body which contract at different speeds and strengths. This is linked to the functional capacity of a muscle in terms of their usage as some body parts work heavy than others (J. A. Smith *et al.* , 2023). Different types of muscles fibers are categorized based on their speed of contraction and aerobic-anaerobic characteristics. Mainly there are three types of muscles cells known as slow oxidative (Type I) cells, fast oxidative (Type IIa) cells and fast glycolytic (Type IIx) cells (Murgia *et al.* , 2021; Rome *et al.* , 1988). The relative abundance of these muscles vary from specie to specie and also with exercise and trainings (Zhelankin *et al.* , 2023).

1.2.1 The fast and slow contracting fibers depend on speed of their energy metabolism and ATPase activity

The speed of a muscle fiber depends on two factors: the load it lifts and its myosin ATPase activity. With a higher myosin ATPase activity in a muscle fiber, ATP split with more efficiency and therefore high amount of energy is made available for contracting fiber. In case of a slow contracting fiber ATP splitting enzymes function at low pace compared to a fast-contracting fiber (Bloemberg *et al.* , 2012; Pellegrino *et al.* , 2003).

Muscles contain heterogeneous form of fibers whose differential abundance determines a muscle fiber type. Glycolytic muscles are fast twitching (the contraction of a single muscle fiber innervated by an action potential) and the majority of fibers get their energy from glycolysis while oxidative muscles contain both fast (type I) and slow (type IIa) twitching (Schiaffino *et al.* , 2011) and acquire their energy through oxidative phosphorylation (Bottinelli *et al.* , 1999; Pellegrino *et al.*, 2003).

Glycolytic muscles appear whitish while oxidative muscles appear reddish in colour. The reddish colour of oxidative muscles is due the rich supply of blood

vessels because of high requirement of oxygen for energy production in contrast to glycolytic muscles where energy is made available through glycolysis in the absence of oxygen. Glycolytic muscles are less tolerant to fatigue because of less availability of ATP molecules. Contrarily, oxidative muscles have considerable stores of ATP energy molecules making them able to cope with long lasting contractions (Khodabukus, 2021; M. D. Zumbaugh *et al.* , 2022; Morgan D Zumbaugh *et al.* , 2022). Any insult to skeletal muscles can bring abnormal function and activity and thereby effect whole organism (Torres *et al.* , 2015).

1.3 Skeletal muscle injuries

Skeletal muscle injuries contribute to global health burden and are characterized by poor lifestyle, morbidity, loss of an organ and even death. These injuries are mainly divided into two types: pathological injuries and physiological injuries (Anderson, 2022; Rahman *et al.* , 2021). The physiological injuries may occur due to overuse, exercise or atrophy while pathological injuries may happen due to military combat, accidents, chemical exposures (barium chloride), and other toxins such as snake venom (cardiotoxins) (Stephen E Alway *et al.* , 2023). A few of these injury types have been discussed in detail in the coming sections.

1.3.1 Contraction-induced injury

The skeletal muscle injury may be caused by the eccentric contractions in which muscle are stretched during the contraction leading to sudden arrest of muscle strength. Such an injury can be caused by intense exercise or downhill running and are characterized by muscle swelling, soreness, high level of serum creatine kinase (CK), enhanced membrane permeability, muscle strength heterogeneity, proteolysis, and mitochondrial dysfunction (Lavender *et al.* , 2006; Liao *et al.* , 2010; Sewright *et al.* , 2008).

1.3.2 Volumetric muscle loss injury

The injuries in which a large part of muscle is removed through surgery or other traumatic injuries including explosive blasts, military combats is known as volumetric muscle loss (VML) injury (Danelson *et al.* , 2019; Grimm *et al.* , 2019). VML causes lifelong disability from immense impairment of muscle activity, neuromuscular dysfunction, and limited muscle regeneration after injury (Greising *et al.* , 2020). In addition, it causes a persistent reduction in

mitochondrial energy capacity which is the main cause of poor muscle functionality (Greising *et al.* , 2016; Greising *et al.* , 2018; Rivera *et al.* , 2016; Southern *et al.* , 2019).

1.3.3 Skeletal muscle burn injury

Burn injuries of skeletal muscles can occur by heat, cold, radiation, friction, electricity, and chemicals. Severe burn injuries initiate hyper-metabolism in the body that result in an increase in ATP consumption reactions (Knuth *et al.* , 2021). Burn injuries to other body tissues also affect skeletal muscles because the state of hyper-metabolism mobilizes amino acid stores from skeletal muscles to aid wound healing. Similarly, body weight starts to reduce due to esterification and gluconeogenesis process to enhance energy expenditure. Besides, burn injury raises an acute apoptotic response, severe uncoupling and reduced mitochondrial respiration (Porter *et al.* , 2016). Disruption of cell membranes due to injury causes mitochondrial permeability pore (mPTP) opening and ROS elevation (Wagatsuma *et al.* , 2011).

1.3.4 Biotoxin-induced skeletal muscle injury

Biotoxins are animals-based substances that can damage skeletal muscles. Different types of biotoxins affect different part of skeletal muscles such as neuromuscular junction, plasma membrane, myofibrils and mitochondria (Mahdy, 2019). For example, Cardiotoxin (CTX) induces depolarization and degeneration of muscle cell plasma membrane (Harris, 2003), and therefore activate Ca^{2+} dependent pathways that trigger the activation of proteases causing mitochondrial dysfunction (Langone *et al.* , 2014).

1.3.5 Ischemia reperfusion injury

The ischemia is referred to inadequate flow of blood to a skeletal muscle that result in shortage of oxygen and nutrients. Whereas reperfusion of blood to ischemic skeletal muscle and the following injury is called ischemia reperfusion injury (IRI). This is characterized by loss of muscle viability and function. Both phases of ischemia and reperfusion trigger severe inflammatory response causing damages at cellular as well as systemic level. Thus, IRI can cause damage to an organ or whole limb, and even sometimes lead to death (Barnig *et al.* , 2022; Finlay *et al.* , 2021). The stress of reactive oxygen species (ROS),

ionic imbalance and activation of neutrophils are mainly responsible for the damaging effect at local and systemic level of IRI (Guo *et al.* , 2019; J. K. Smith *et al.* , 1989).

IRI impairs mitochondria and initiates reduction in mitochondrial respiration capacity and expression of mitochondrial enzymes. Indeed, impaired mitochondria has a key role in reduced muscle functionality (Orfany *et al.* , 2020). Reperfusion causes cellular damage via mitochondrial Ca²⁺ overload, high ROS and reduced production of ATP (Mansour *et al.* , 2012). This is followed by release of cytochrome C thereby enhanced autophagy and cell death (Call *et al.* , 2017).

1.3.6 Skeletal muscle atrophy

Skeletal muscle atrophy is defined as the decrease in muscle mass and strength which happens mainly due to an imbalance in protein turnover rate i.e. proteins degradation surpasses proteins synthesis (L. Yin *et al.* , 2021). Muscle atrophy may originate from either inherited or acquired conditions (Schiaffino *et al.* , 2013; Vainshtein *et al.* , 2020).

The inherited disorders, either genetic or congenital are characterized by progressive atrophy, metabolic dysfunction, muscle rigidity and spasm. For example, muscular dystrophies, congenital myopathies and common mitochondrial myopathies. (de Winter *et al.* , 2017; Liang *et al.* , 2020b). Muscle atrophy can also be acquired from pathological or physiological conditions for example age related sarcopenia (N. E. Johnson, 2019), diabetes, kidney disease, obesity (Kunz *et al.* , 2020), heart failure, burns and trauma (R. J. Johnson *et al.* , 2007).. In addition, poor diet, lifestyle and muscle disuse due to long bed rest or coma may also lead to muscle atrophy (Yin *et al.*, 2021).

1.3.6.1 Molecular mechanisms of skeletal muscle atrophy

Although the overall mechanism of muscle atrophy is not fully elucidated, the balanced rate of protein synthesis verses protein degradation gets disturbed by some upstream signals including ROS accumulation (Silva *et al.* , 2015), inflammation, impaired mitochondria, and downstream components including autophagy lysosome ubiquitin proteasome system (Aniort *et al.* , 2019, activation of caspases (Connolly *et al.* , 2020) and calpains (Sorimachi *et al.* ,

2011). These systems are interdependent and may work in a complex combination to elicit complete degradation of proteins leading to skeletal muscle atrophy (Vainshtein *et al.*, 2020).

1.3.6.2 Upstream signaling pathways of skeletal muscle atrophy

Various diseases that cause muscle atrophy have common factors of oxidative stress, mitochondrial dysfunction and inflammation, which are working together to contribute towards impaired skeletal muscle proteostasis (Oba *et al.*, 2020). The decrease in healthy mitochondria and elevated ROS reduce protein synthesis and enhance proteolysis leading to muscle atrophy. Similarly, chronic inflammation also contribute to dysregulation of protein metabolism via interaction of various cytokines such as, IL-6 and TNF- α . For instance, IL-6 is known to inhibit JAK-STAT3, ERK and PI3K/Akt pathways and therefore lead to protein degradation (Silva *et al.*, 2015). TNF- α enhances protein degradation while contrarily inhibits protein synthesis in aging related disease and particularly in cancer (Zhou *et al.*, 2016).

1.3.6.3 Calpains and caspases

Calpains are Ca²⁺-dependent enzymes involved in proteolysis of skeletal muscles (Sorimachi *et al.*, 2011). In skeletal muscles, the elevated resting cytoplasmic Ca²⁺ act as a trigger for calpain activation and the following proteolysis (Ono *et al.*, 2016). These enzymes can degrade several proteins such as, cytokines, phospholipases, various transcription factors, membrane proteins, and several muscle proteins such as, α -actinin, desmin and Z-disk anchoring proteins (Friedrich *et al.*, 2015). Moreover, calpains also cause mitochondrial dysfunction and oxidative stress in skeletal muscles (Munkanatta Godage *et al.*, 2018).

Caspases are another family of proteases that are not only involved in mediating different cell deaths like apoptosis, necroptosis and pyroptosis but also induce other harmful pathways such as inflammation and differentiation (Connolly *et al.*, 2020). Studies suggest that TNF- α triggers signalling cascade that cleaves and activate procaspase-8 to caspase-8, which further cleaves and activates procaspase-3 to caspase-3, hence forth, degrade actin and myosin proteins of skeletal muscles and as a consequence cause loss of muscle strength (Friedrich *et al.*, 2015).

1.3.6.4 Ubiquitin-proteome system

The ubiquitin-proteasome system (UPS) has a critical role in proteolysis of muscle atrophy (L. K. Chen *et al.* , 2020). There are various disease conditions including diabetes, cancer, fasting, denervation, and renal failure that led to UPS up regulation thereby causing muscle atrophy (Lecker *et al.* , 2004). UPS involves the ubiquitination of target proteins, destined for degradation. This process is facilitated by E1, E2, and E3 ubiquitin ligase enzymes. E3 ligases are rate-limiting enzymes in ubiquitin conjugation and provide specificity to the UPS. Skeletal muscles have specific E3 ligases called MuRF1 and Atrogin-1 which are up regulated in muscle atrophy causing protein imbalance. MuRF1 is involved in the degradation of skeletal muscles proteins while Atrogin-1 targets proteins that promote growth and survival (Aniort *et al.* , 2019; Lecker *et al.*, 2004).

Different signaling pathways and factors are known to be involved in different catabolic conditions as shown in the **Fig. 1.2**. For instance, MuRF1 induces aging and glucocorticoid-induced skeletal muscle atrophy while it does not have a role in fasting and microgravity-induced atrophy (Bodine *et al.* , 2001; Vainshtein *et al.*, 2020). Similarly, Atrogin-1 has only role in starvation-triggered atrophy (Sandri *et al.* , 2013; Sartori *et al.* , 2013; Vainshtein *et al.*, 2020). These ligases are considered as master genes of muscle atrophy (Atrogens). Besides, there are also some other genes involved in muscle atrophy. Scientists have predicted over 640 E3 ligases in the human genome and there are still more to be identified (Cohen *et al.* , 2012). Among these Trim32 is involved in degradation of thin filaments and z-band proteins whereas, TRAF6 act upstream of NF-kB which act in stabilizing ULK1 activity (autophagy inducer) (Paul *et al.* , 2010). Although, the UPS has a great part in muscle atrophy that is for degrading high part of proteins, it is not involved to degrade intact myofibrils and organelles, emphasizing the presence of other systems contributing to the complex interplay among different proteolytic systems (Nazio *et al.* , 2013; Vainshtein *et al.*, 2020).

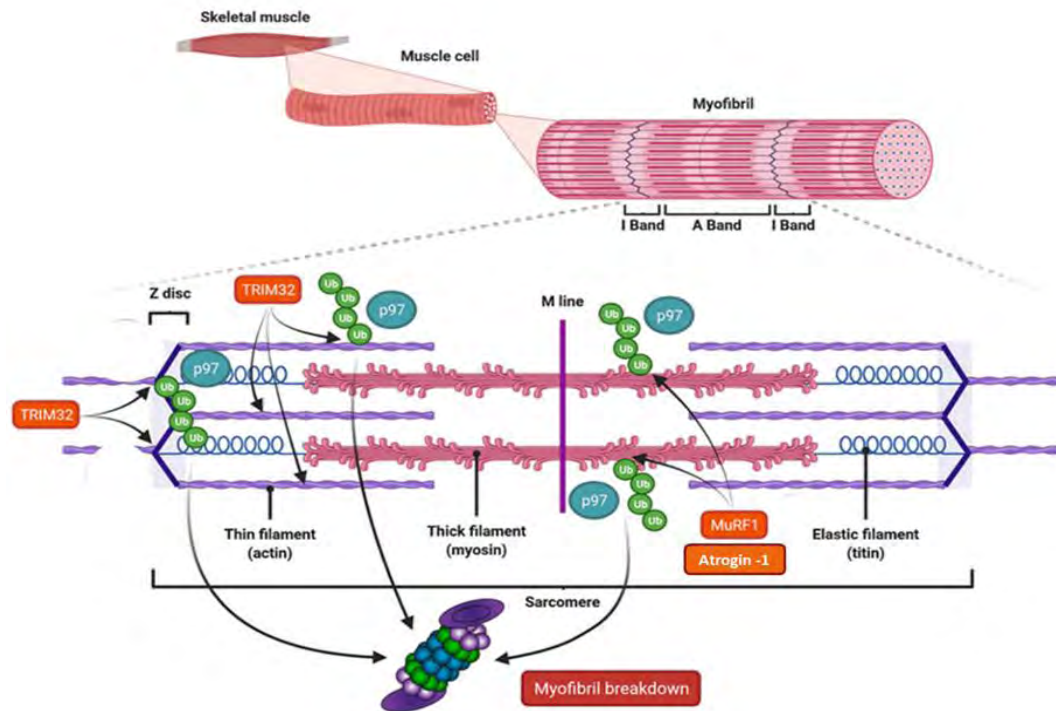


Fig 1.2. Ubiquitin-proteasome pathway of skeletal muscle atrophy. *E3 ligases like MuRF1, Atrogin-1 and TRIM32 ubiquitinate thick and thin filaments and target these to proteasome degradation (Haberecht-Müller et al. , 2021).*

1.3.6.5 Autophagy-lysosome system

Autophagy lysosomal system plays critical role in regulation of skeletal muscles (Masiero *et al.* , 2009). Autophagy can be defined as the transfer of cellular components and organelles to lysosome for degradation. It regulates homeostasis in skeletal muscles by removal of damaged components of muscles fibers while the inhibition of this system triggers muscle degradation. Thus, the imbalance in this system ends up in muscle atrophy (McGrath *et al.* , 2021).

Autophagy related genes called Atgs are involved in recognition and membrane commitment of cargo. Despite the initial belief of nonselective autophagy system, it is involved in selective degradation of cellular components (Ekelund *et al.* , 2016). Indeed, autophagy can select and eradicate dysfunctional mitochondria or any abnormal protein-aggregates. Certain proteins that act as adapter proteins like p62 and Bnip3 bind autophagosomes via LC3, and

dysfunctional organelles which are not labelled by ubiquitin chain, (**Fig. 1.3**), (Castets et al. , 2013).

Impairment in autophagy leads to muscle degeneration and weakness because normally it is responsible for constantly providing metabolites to sustained cellular metabolism, washing out damaged cellular components, and promoting regeneration and resistance to stress (Castets *et al.*, 2013). Furthermore, dysregulation of autophagy can cause increased oxidative stress, accumulation of dysfunctional mitochondria, weakness and finally atrophy (Castets *et al.*, 2013; Tezze *et al.* , 2017).

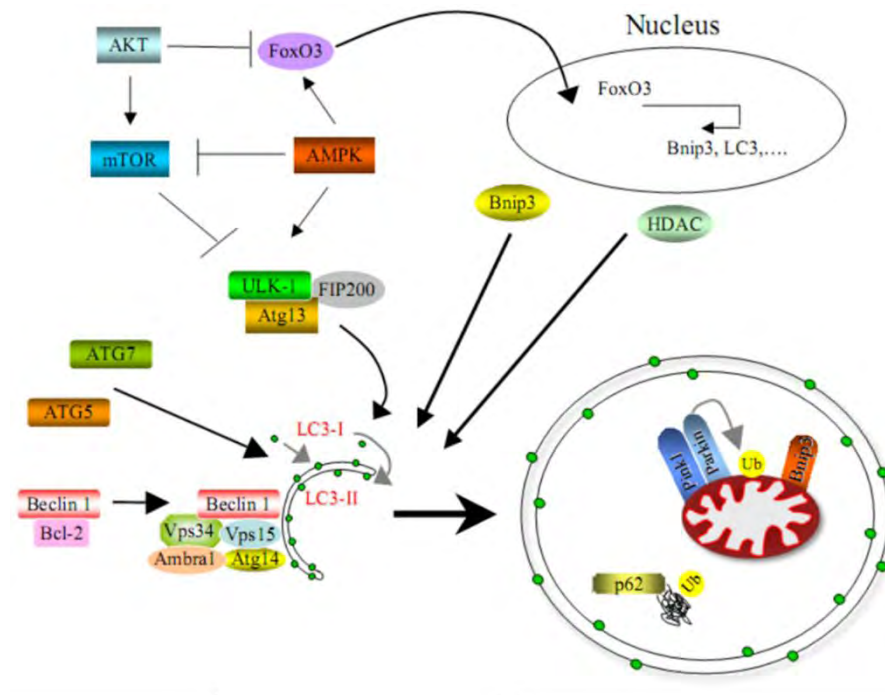


Fig. 1.3 The formation of autophagosome via autophagy lysosome system in skeletal muscle atrophy. Akt act as negative regulator of autophagy rapidly through inhibition of FoxO3 and via mTOR pathway for long term. In downstream pathway, mTOR inhibit Atg 13 and ULK1 to repress autophagy. AMPK is autophagy initiating protein that trigger autophagy either through transcriptional activation of Beclin 1, Atg 12, bnip 3 and LC3 via translocation of FoxO3 to nucleus and autophagosome formation through activation of ULK1. Some proteins are directly involved in autophagy like Atg5 and Atg7 promoting muscle skeletal muscle atrophy. Histone deacetylase (HDAC) act as autophagy enhancer.(Grumati et al. , 2012).

1.3.7 BaCl₂-induced skeletal muscle injury

BaCl₂ has advantage over other myotoxic chemicals to study skeletal muscle regeneration due to its easy usage and causes injury without affecting satellite stem cells (MSCs). Ba²⁺ ion block K⁺ channels and depolarizes plasma membrane leading to activation of voltage gated calcium channels in the sarcolemma (Cho *et al.* , 2017; Flucher *et al.* , 2017). Therefore, the elevation of Ca²⁺ in myoplasm via release from sarcoplasmic reticulum and from extracellular fluid influx, cause lysis of contractile proteins and disruption of sarcolemma (Turner *et al.* , 1988). Similarly, BaCl₂ also causes damage to neuronal axons and micro vessels (Aaron B Morton *et al.* , 2019).

BaCl₂-induced depolarization of the myofibers (Maqoud *et al.* , 2017) and ensuing Ca²⁺ rise in the cytoplasm and mitochondria may lead to excessive production of ROS which disrupts the integrity of actomyosin proteins (Morton *et al.* , 2019). Moreover, high Ca²⁺ levels activate proteases such as calpains and cleave various skeletal muscle proteins for example, titin, nebulin, and α -II-spectrin (Goll *et al.* , 2003) . This chemical has also demonstrated its degenerating impact on motor axons that lie with in the vicinity of exposed muscle (Torigoe *et al.* , 1996).

Skeletal muscle injuries have very diverse risk factors and almost all those factors induce mitochondrial dysfunction. Indeed, mitochondrial health is very critical for normal skeletal muscle health. Thus, impaired mitochondria result in cellular energy deficit and modulation of cell disrupting pathways, consequently leading to reduced regeneration process and full recovery after injury. (Michelucci *et al.* , 2021).

1.4 Mitochondrial dysfunction in skeletal muscle injuries

Skeletal muscle requires substantial amount of energy ATP to meet high demands of skeletal muscle activities. This energy is provided by electron transport chain through oxidative phosphorylation (OXPHOS) (Ulger *et al.* , 2022). Following skeletal muscle injuries mitochondria damage and their membrane potential ($\Delta\Psi_m$) is lost resulting in a lack of energy to rescue muscle injury. There are a number of factors that contribute to mitochondrial dysfunction in muscle injuries such as ROS elevation, Ca²⁺ overload and

imbalanced mitochondrial dynamics (J. C. Liu *et al.* , 2020; Rodney *et al.* , 2016).

1.4.1 Ca²⁺ overload

Ca²⁺ is a second messenger that plays key roles in regulation of skeletal muscle function. Mitochondria need a steady influx of Ca²⁺ for the regulation of normal metabolism in muscle cells (Bravo-Sagua *et al.* , 2017). Mitochondrial Ca²⁺ homeostasis regulates the size, activity and metabolism of skeletal muscles (Gherardi *et al.* , 2019). However, the abrupt increase of Ca²⁺ influx in mitochondrial matrix leads to the opening of mPTP via the increased activity of cyclophilin D, a regulatory protein responsible for activation of mPTP. The opening of this nonspecific pore allows various types of substances to enter mitochondria which as a consequence, cause mitochondrial swelling and the following rupture of both inner and outer mitochondrial membranes, (**Fig. 1.4**) (Stephen E Alway *et al.*, 2023).

Moreover, the membrane permeabilization of mitochondria also ends up in release of pro-apoptotic components such as cytochrome C, thus, loss of bioenergetics ability and activation of cell death pathways (Morris *et al.* , 2021). Additionally, Ca²⁺ overload has also been demonstrated to degenerate mitochondrial electron transport chain protein complex II causing cell death, (**Fig. 1.4**) (Hung *et al.* , 2017)

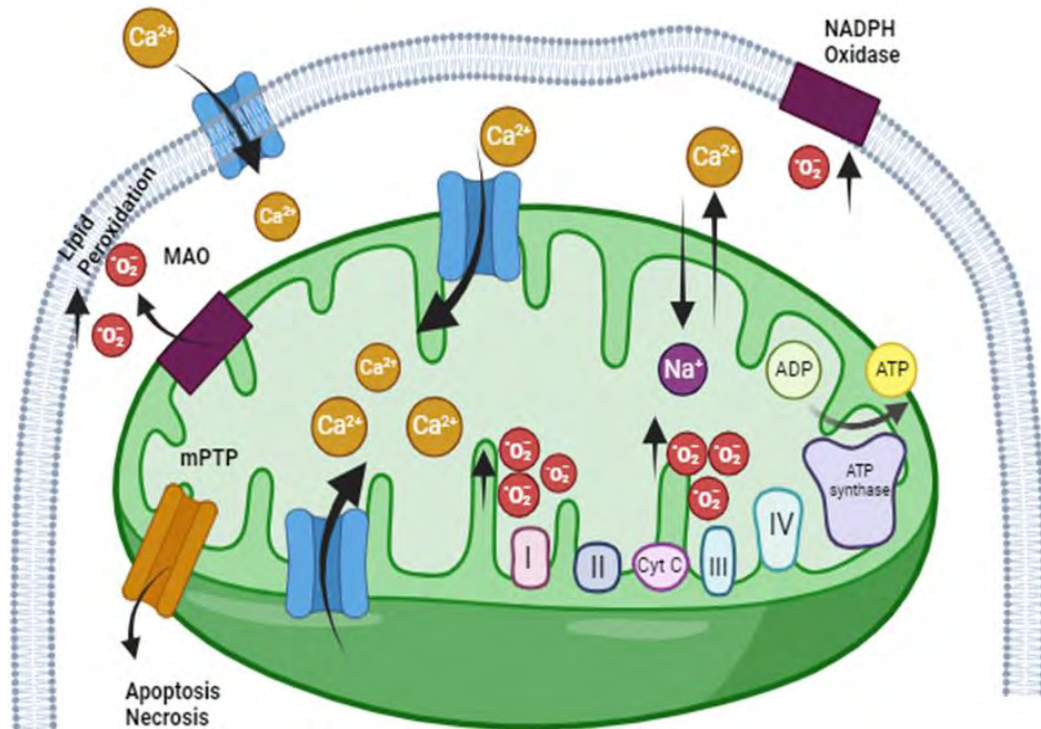


Fig. 1.4 Mitochondrial stress due to elevated ROS and Ca^{2+} . High levels of both ROS and Ca^{2+} cause opening of mitochondrial permeability transition pore (mPTP) leading to mitochondrial swelling, reduced OXPHOS, lipid peroxidation of plasma membrane, and cell death activation, (made by Biorender.com).

1.4.2 Oxidative stress

Mitochondrial OXPHOS complex involves series of enzymes that transfer electrons from substrates (carbohydrates and fats) to oxygen molecule and produce ROS. In this way, mitochondria act as one of the major sources of ROS (Jones, 2008; Murphy, 2009; Quinlan *et al.*, 2013). In skeletal muscle injuries, the rate of oxidation reaction increases and result into premature leakage of electrons towards oxygen leading to formation of high-level ROS-superoxide radicals. Elevated ROS is known to destabilize cellular membrane by lipid peroxidation and thereby leading to efflux of cellular contents (Al-Menhali *et al.*

, 2020). Besides, in elevated Ca^{2+} environment, an increase in ROS level also ends up in mPTP opening (Crompton *et al.* , 1987; Robichaux *et al.* , 2022). Moreover, ROS-dependent opening of mPTP further increases ROS in the cytosol (Zorov *et al.* , 2000) and thereby causes mitochondrial swelling and impairment even in the presence of low Ca^{2+} levels (**Fig. 5**) (Cervinková *et al.* , 2007; Seidlmayer *et al.* , 2015).

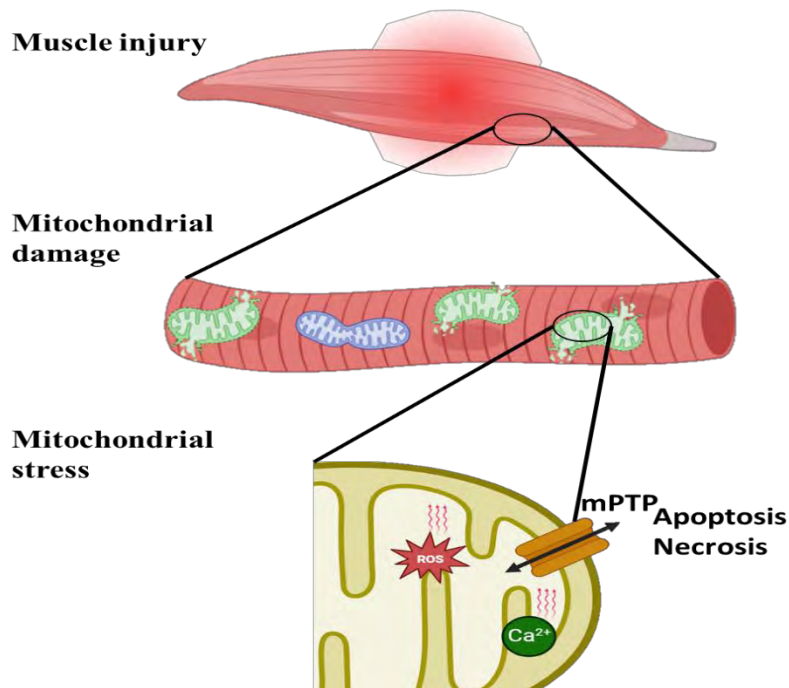


Fig. 1.5 Skeletal muscle injuries cause mitochondrial stress by elevated ROS and Ca^{2+} that is followed by mPTP opening leading to cell death via apoptosis and/or necrosis (Designed by Biorender).

1.4.3 Mitochondrial dynamics

Mitochondrial dynamics including fission and fusion are critical to cellular activities (Abel, 2018). Genes involved in mitochondrial fusion (mitofusin 1 and 2) and fission (DRP1, MID49/51, and MFF) are known to regulate mitochondrial dynamics. A dysregulated mitochondrial fusion and fission trigger distinct inflammatory responses in skeletal muscle injuries by elevating levels of pro-inflammatory cytokines (IL-6, IFN β 1, and TNF α) (Favaro *et al.* , 2019; Hamel *et al.* , 2021). Mitochondrial fragmentation is known to initiate TLR9-dependent

inflammation, an increase in IL-6 levels that causes loss of muscle cells (Irazoki *et al.* , 2023). Together, data reveals that changes in mitochondrial morphology contribute to inflammatory profile which consequently affect muscle mass and response to regeneration after an injury.

1.4.4 Mitophagy

Mitochondrial dysfunction accompanies the loss of $\Delta\psi_m$ and kicks on mitophagy (autophagic clearance of mitochondria) via a cascade of events that are linked to inflammatory response (Irazoki *et al.* , 2022; Paez *et al.* , 2023). Indeed, damaged mitochondrial clearance is necessary for balanced proteostasis in healthy muscles (Sliter *et al.* , 2018). The mitochondrial membrane potential is disrupted by various factors including sarcopenia, elevated ROS level and skeletal muscle injuries. These events can cause the sequestration and stabilization of PTEN-induced kinase 1 (PINK1) at outer mitochondrial membrane (OMM) (Fallaize *et al.* , 2015). PINK1 further recruit Parkin, a ubiquitin ligase which is usually present in cytosol as inactive molecule until a pathological environment is generated. It ubiquitinates mitochondrial membrane proteins and targets it for degradation via mitophagy (Sarraf *et al.* , 2013; Slavin *et al.* , 2022).

1.5 Therapeutic strategies to repair skeletal muscle injuries

Mitochondrial dysfunction is one of the common factors for most skeletal muscle injuries. Thus, making it the main target of pharmacological approaches to treat muscle injuries (Andreux *et al.* , 2013; Murphy *et al.* , 2000; Wallace *et al.* , 2010). Mostly these approaches focus on enhancing energy capacity, reducing, and eliminating ROS, and triggering mitochondrial biogenesis (Lang *et al.* , 1997; Liet *et al.* , 2003).

1.5.1 Natural products as therapeutics

Several naturally occurring compounds are known to enhance mitochondrial capacity of ATP synthesis such as dimethylglycine, co-enzyme Q, and idebenone (Lerman-Sagie *et al.* , 2001; Liet *et al.* , 2003). Antioxidants like N-acetylcysteine reduce mitochondrial ROS levels and enhance mitochondrial respiration capacity in skeletal muscle injuries (Lejay *et al.* , 2018). Elamipritice (ELAM), a natural compound that binds with cardiolipin in the inner mitochondrial membrane. Its binding stabilizes the structure of cardiolipin and

thereby promote cristae formation. Thus, ELAM prevents mitochondrial oxidative stress and improves the oxidative capacity of mitochondria leading to generation of high ATP energy molecules (Roshanravan *et al.* , 2021). Similarly, tetramethylpyrazine is another plant-based compound known for alleviating the effect of muscle atrophy. This compound reduces ROS levels and Ca²⁺ overload and therefore leads to recover proteolytic and apoptotic balance (Hu *et al.* , 2017). Salidroside inhibits the elevated ROS production and alleviates skeletal muscle atrophy (Z. Huang *et al.* , 2019).

There are several other natural compounds acting as potent antioxidants that can clear the excessive ROS. For example: 1) polyphenols can inhibit oxidative stress and recover mitochondrial dysfunction (Salucci *et al.* , 2020), 2) Resveratrol reverses mitochondrial dysfunction by down regulating oxidative stress and enhances mitochondrial activity (Y. Huang *et al.* , 2019). Some compounds amplify mitochondrial biogenesis such as, Mours alba L. extract increases the activation of p-AMPK and PGC-1 α pathway which is involved in mitochondrial biogenesis thus, greater mitochondrial content that provides enough energy to relieve skeletal muscle injuries (Meng *et al.* , 2020).

1.5.2 Other therapies

Targeting muscle atrophy genes: An isoflavone analogue, puerarin positively affects skeletal muscle strength and mass in diabetes-induced skeletal atrophy (M. J. Kim *et al.* , 2023). In addition, it reduces mRNA expression of atrophy-causing genes (Atrogen1 and MuRF1) and thereby, increases muscle-fiber cross-sectional area (M. J. Kim *et al.*, 2023). Moreover, soy isoflavones, are plant-based products which inhibit the accumulation of fats and improve skeletal muscle mass (Beekmann *et al.* , 2015; Kurrat *et al.* , 2015).

Physical exercise: Studies show that regular exercise improve muscle health with increased life expectancy and reduced morbidity in life during aging (Chakravarty *et al.* , 2008; Roberta Sartori *et al.* , 2021). AMPK and PGC1 α regulation are critical to exercise-induced adaptations. Over activation of AMPK causes muscle wasting and weakness while expression of PGC1 α enhances muscle size (R. Sartori *et al.* , 2021). Specifically, endurance exercise like push-ups, chin-ups, dumbbells etc. increase anabolism while decrease catabolism of skeletal muscles (Schoenfeld, 2010). Endurance exercise also called aerobic

exercise prolongs cardiovascular health and inhibits pro-inflammatory cytokines (Pranoto *et al.* , 2023). Additionally, it inhibits myocytes autophagy and enhances the proliferation of satellite cells (Moreira *et al.* , 2020; N. N. Wu *et al.* , 2019).

1.6 Mitochondrial transplantation therapy

One of the innovative therapeutic strategies against mitochondrial dysfunction-associated disorders is the transplantation of exogenous mitochondria in the diseased organ. Mitochondrial transfer in injured skeletal muscles have shown some promising results. Direct mitochondrial transplantation is possible based on two evolutionary evidences; one is its endosymbiotic behaviour, and the second, is its retained bacterial ability to enter a cell (M. J. Kim *et al.*, 2023). Mitochondria isolated from different sources (autogenic, allogeneic or xenogeneic) have been used for therapeutic purposes which ameliorated mitochondrial dysfunction and restored normal metabolic activities (C.-Y. Chang *et al.* , 2019; Z. Liu *et al.* , 2022; Tria *et al.* , 2021). Mitochondrial transplantation has been carried out both in vitro and in vivo studies of skeletal muscle injuries.

1.6.1 In vitro mitochondrial transplantation

Several techniques have been demonstrated to transplant the exogenous mitochondria into target cells or tissues and are briefly described below:

Co-Incubation method: The first in-vitro mitochondrial transplantation was carried out in 1982 by co-incubation method, suggesting that purified mitochondria from human fibroblasts having mutations of chloramphenicol (CAP) and efrapeptin (EF) resistance, induce antibiotic resistance when co-incubated with antibiotic sensitive dysfunctional human cells (Clark *et al.* , 1982).

Direct microinjection: Isolated mitochondria from CAP-resistant cell line, successfully produce resistance in mitochondrial DNA (mtDNA) depleted 143B human osteosarcoma cell lines through direct injection. This proves the phenomena of uptake of exogenous mitochondrial DNA contents after successful transplantation when analysed on mtDNA polymorphisms (King *et*

al., 1988). The data suggests that mitochondria transplantation can repopulate mitochondrial depleted cell lines (King *et al.*, 1988).

Clark and shays technique: A penetrating peptide (Pep-1) is conjugated with mitochondria which has the ability to cause pores in host cell plasma membrane. These pores facilitate mitochondrial transfer. The transferred mitochondria co-localize with host cells mitochondria and recover their membrane potential (J.-C. Chang *et al.*, 2017).

MitoCeption method: This method is based on the application of centripetal force through which mitochondrial suspension is isolated via differential centrifugation method and are added to cultured cells in a petri dish. Cells are centrifuged to facilitate the transfer of added mitochondria (Cabrera *et al.*, 2019; Caicedo *et al.*, 2015).

Photothermal technique: Using this technique, mitochondrial transfer is made possible via opening of plasma membrane by applying biophotonic-laser-assisted surgery tool (BLAST). The rapid and parallel cargo of isolated mitochondria is transferred into the recipient cells (Y.-C. Wu *et al.*, 2015).

Magnetomito transfer: This is a novel technique that employs magnetic beads to label mitochondria. The labelled mitochondria are carried to the host cells via a magnetic plate. Similarly another method has been developed called Mitopunch which contain a device driven by pressure named as Mitopunch that transfers mitochondria to recipient cells seeded on porous polyester membrane (Sercel *et al.*, 2021).

FluidFM: This is single cell technology to perform mitochondrial transplantation between living cells. It maintains integrity of mitochondria and cells as well. This technique is less invasive because it uses special probes to access into cell and flow of fluids in order to extract and then inject mitochondria in recipient cell (Gäbelein *et al.*, 2022).

EV-mediated MT method: Naked mitochondria transplantation can trigger immune response and cause toxicity that can compromise mitochondrial integrity. The encapsulation of isolated mitochondria in extra cellular vesicles

(EVs) can increase the preservation time and protect mitochondrial integrity during transplantation (Peruzzotti-Jametti *et al.* , 2021).

1.6.2 In vivo mitochondrial transplantation

In addition to in vitro studies of mitochondrial transplantation (MT), mitochondrial transplantation has also been performed in animal models including mice and rats. First ever in vivo MT study was performed in 2009 using model of heart ischemia-reperfusion of rabbit (McCully *et al.* , 2009). This study highlighted that rabbit cardiac ischemia reperfusion injury is improved after transplantation of exogenous mitochondria isolated from left ventricular tissue of healthy animal. Moreover cardiomyocytes have the ability to uptake exogenous mitochondria within 2 hours after injection (Masuzawa *et al.* , 2013).

Furthermore, MT significantly reduces markers that are elevated in cardiac ischemia injury, which include creatine kinase-MB and Troponin I. Similarly, MT also reduces pro-apoptotic proteins of Caspase-3 as well as infarct size (Masuzawa *et al.*, 2013). In case of heart there are two types of methods for in vivo MT: (1) MT via direct injection to injury site (**Fig. 1.6**), and (2) administration of mitochondria thorough coronary arteries in case of myocardial IR injury. However, MT locally into injury site is proved to be more effective and efficient in myocardial IR injury alleviation (Cowan *et al.* , 2016).

1.7 Exogenous mitochondrial sources for in vivo MT

Multiple sources of exogenous mitochondria are used to perform MT in *in vivo* studies. In some studies mitochondria is isolated from brain tissues and MT is performed in cardiac IRI and depression animal models (Hayashida *et al.* , 2023; Y. Wang *et al.* , 2019). In addition, mitochondria has been derived from cultured cell lines such as PC-12 (pheochromocytoma cell), N2a (neuroblastoma) and mNSC (motor neurons), and implemented through direct MT in spinal cord and cerebral ischemia injuries through carotid artery (Gollihue *et al.* , 2018; Xie *et al.* , 2021). Similarly, in a study, MSCs (mesenchymal stem cells) are used as source of mitochondria to transplant into a kidney disease rat model (Kubat *et al.* , 2021). Moreover, mitochondria can also be purified from skeletal muscles, as in a study mitochondria from pectoralis major muscles and MT taken place in mice myocardial IRI (Jia *et al.* , 2022).

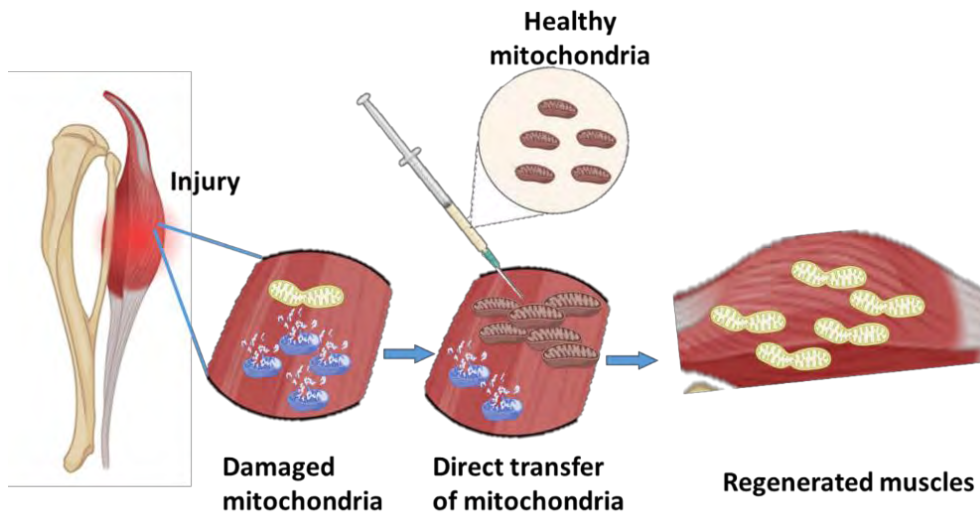


Figure 1.6 Mitochondrial transfer to the injured skeletal muscle. *Healthy isolated mitochondria transferred to injured muscle contribute to muscle cell regeneration and alleviation of injury (Designed by Biorender).*

1.8 MT in skeletal muscles injuries

Studies are performed for MT in several animal tissues such as brain, liver, lungs and skeletal muscles (Yamada *et al.*, 2020). However, there are three reported studies so far in which mitochondria have been transplanted in skeletal muscles undergoing muscle injuries, including IRI (**Fig. 1.6**), muscle atrophy and myotoxic injury. In all these studies mitochondria were isolated through centrifugation method followed by local administration in muscles. The transplantation of xenogeneic mitochondria isolated from Umbilical cord mesenchymal stem cells (UC-MSCs) in dexamethasone-induced skeletal muscle atrophy rat model, enhances mitochondrial health, muscle strength and mass. In addition, MT down regulates expression of atrophy causing genes (Atrogin 1 and MuRF1) along with enhancing activation of muscle regenerating signaling pathways such as, AKT/FoxO signaling pathway (M. J. Kim *et al.*, 2023). Similarly, the skeletal muscle derived mitochondria and the following MT in IRI muscles allows mitochondrial up take by cells which improves ATP content and decreases muscle necrotic size (Orfany *et al.*, 2020). Moreover, liver derived intra venous MT in a BaCl₂-induced myotoxic injury improves muscle structure

and function. Furthermore, MT increase muscle mass, strength, and muscle fiber cross section area (CSA) (S. E. Alway *et al.* , 2023).

Aim and Objectives

The aim of this study was the evaluation of exogenous mitochondrial transfer as a therapeutic strategy in mice skeletal muscle injuries with the following objectives.

- a) The development of skeletal muscle atrophy model using dexamethasone
- b) The establishment of skeletal muscle myotoxic injury model using BaCl₂
- c) MT in injured skeletal muscles to assess its effect on dexamethasone and BaCl₂-induced muscle injuries.

2. Material and Methods

2.1 Ethical approval of the study and animal handling

This study involved the use of Swiss albino BALB/c mice for the development of mice models of muscle atrophy and muscle injury. To ensure the ethical conduct of the study, ethical approval was sought from the institutional bioethical committee (IBC) of Quaid-i-Azam University Islamabad. Mice were kept in the animal facility to grow and breed under facilitative conditions provided with ad libitum access to enough water and diet.

2.2 Mitochondrial isolation

Mitochondria were isolated from the liver of healthy mice as described in several studies (Orfany *et al.*, 2020). Mice were anaesthetized with chloroform and an incision was made in the abdominal side extending toward the chest. The liver was isolated carefully and immediately transferred to a petri dish containing 1X PBS buffer (phosphate buffered saline: 137mM NaCl, 1.8 mM KH₂PO₄, 2.7mM KCl and 10mM Na₂HPO₄). The whole process was carried out on ice-cold conditions. The tissue was washed multiple times thoroughly using PBS to remove any remnants of blood and then transferred to a new petri dish. Liver tissue of 500 mg was minced using surgical blade in 2 ml of homogenization buffer (HB: Sucrose 250 mM, KCl 1.0 mM, EDTA 0.1 mM, Mannitol 250 mM, HEPES 25 mM, and PMSF 100 mM) until a uniform tissue homogenate was obtained devoid of any apparent debris. Next, the tissues were transferred into 15ml glass Teflon homogenizer and 3 ml of HB buffer were further added to generate enough pressure in the homogenizer for efficient cell lysis. The tissue was homogenized for 7 strokes manually to achieve a uniform homogenate. Finally, it was transferred into a pre-chilled 50 ml centrifugation tube (SPL, Korea). All the steps are shown in (Fig. 2.1).

2.3 Enrichment of mitochondrial crude extract via differential centrifugation

Mitochondria were extracted from the minced and homogenized liver tissue using differential centrifugation. The centrifuge (X-30R, Beckman Coulter) was pre-set at 4°C to protect mitochondria from degradation during the whole process of centrifugation. Crude mitochondria were extracted by a three-step

centrifugation process. In the first step, the tissue homogenate was centrifuged at low speed of 500 x g for 10 minutes. At this step, intact cells, cellular debris, and nuclei were settled down leaving an upper layer of supernatant. In the second step, the supernatant was shifted to another tube and centrifuged at a high speed of 3000 x g for 10 minutes. This time the pellet was kept which was supposed to carry large sized mitochondria. The pellet was washed using 2 ml of 1X PBS buffer and recentrifuged again at 3000 x g for 10 minutes. Finally, the obtained pellet containing crude mitochondria was suspended in assay buffer (120 mM KCL, 10mM MOPS, 5mM Glutamate, 5mM Malate, 20mM EDTA) and kept at 4°C until further processing (**Fig. 2.1**).

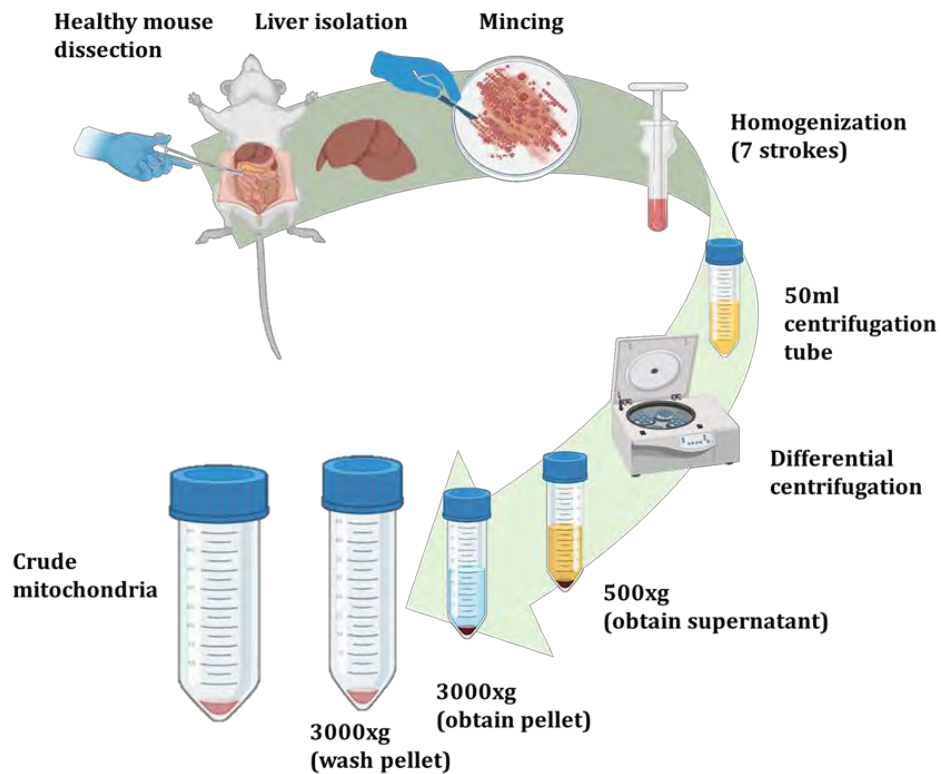


Fig. 2.1. Schematic diagram of mitochondrial isolation from healthy mice liver tissues (Designed by Biorender.com).

2.4 Mitochondrial protein quantification

Mitochondrial protein quantification was carried out using Bradford assay. Mitochondrial suspension was diluted 10 times by adding the assay buffer and then 10 μ l from it was poured in a well of 96-well microplate (Extracene EL-1190-F, South Korea) followed by addition of 200 μ l of 1 x Bradford reagent. The plate was incubated at 37°C for 30 minutes. At the end of the reaction the

absorbance was collected at 595 nm on a spectrophotometer. Mitochondrial protein content was calculated by using the standard curve plotted on Microsoft Excel.

For the preparation of standard solution, Bovine Serum Albumin (BSA) (Carl Roth, Germany) was used. The stock solution of 40mg/ml of distilled water was made and diluted twenty times followed by preparation of seven dilutions further ranging from 0-1.2 $\mu\text{g}/\mu\text{l}$ in a total volume of 100 μl each. 10 μl of blank containing distilled water and the BSA standard solution were poured in 96-well microplate (Extragene, EL-1190-F, South Korea). After an incubation period of 30 minutes at 37°C the absorbance values were measured at 595nm on a spectrophotometer. The absorbance for all BSA standard solutions were corrected by subtracting the blank value. The corrected absorbance values were plotted on a curve to calculate values of mitochondrial crude extract, as shown in Fig. 2.2.

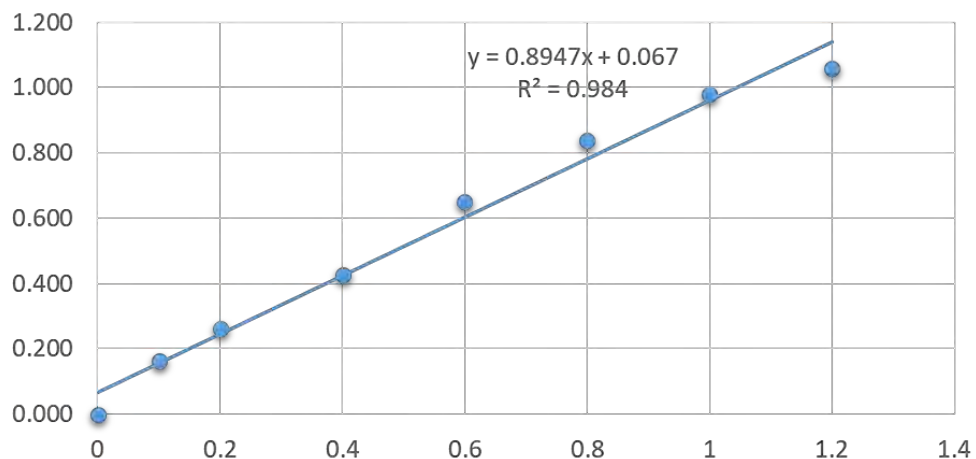


Fig. 2.2. Standard curve for BSA used to find the protein contents of isolated mitochondria.

2.5 Mitochondrial oxygen consumption rate

For assessing the viability of isolated liver mitochondria, oxygen consumption rate (OCR) was measured using Oxygraph+ (Hanstech Instruments Limited, England). To determine OCR, liquid phase calibration was performed before each experiment. It was made sure that the electrode disc was free from any silver chloride or oxides crystals. After initial cleaning steps, electrode disc was assembled by following standard electrode disc preparation steps.

Briefly, 50% saturated potassium chloride (electrolyte) was used to completely dip the silver anode and moistening the platinum cathode. 1.5-2cm³ spacer paper followed by Polytetrafluoroethylene (PTFE) membrane were arranged centrally over the platinum dome. This is followed by placement of the small O-ring around the dome using the membrane applicator tool. The electrode is connected to the power unit and the disc assembly was tested by exhaling breath over the disc. The electrode fitness is tracked by OxyTrace+ software (Hanstech Instruments Limited, England). A large drop in the oxygen level in the chamber is used as indicator of the assembly fitness and proper functioning. After successful electrode testing, large O-ring was placed in the recess around the well (it should not touch with the excess PTFE membrane). At the end, chamber was positioned over the electrode followed by its placement over the power unit of Oxygraph+. 2mL of assay buffer or 0.5µg/mL of freshly isolated liver mitochondria were introduced in the oxygraphy+chamber (carrying PTFE coated magnetic stirrer). The container was sealed by using a standard plunger assembly. The oxygen consumption rate (OCR) in nm/mL/min was measured by using OxyTrace+ for 5 min in the presence or absence of 5mM Glutamate. The data analyzed by calculating the slope of the OCR curve before and after glutamate addition using Excel (Microsoft 365) and GraphPad Prism v5.1 (Graphpad Holdings, USA).

2.6. MTT assay

To check the viability of isolated liver mitochondria, MTT assay was performed. This assay is named after 3-(4,5-dimethylthiazol-2-yl)-2,5-diphenyltetrazolium bromide (MTT) (Serva 20395-03, Germany) which is the water-soluble salt with yellow colour. In viable mitochondria endogenous succinate dehydrogenases reduce MTT tetrazolium into formazan crystals changing its colour from yellow to purple. MTT with 5mg/ml stock was diluted at 1:5 ratio in assay buffer. Next, 5µg/µl of mitochondria was poured into microplate well which was then followed by MTT addition. The plate was incubated in dark for 30 minutes at 37°C. After half an hour the DMSO was added at the same volume as mitochondrial suspension to solubilize formazan crystals. Finally, the reading was recorded on spectrophotometer (Multiskan GO, USA) at 570 nm.

2.7 Mitochondrial transplantation (MT)

After quantification, about 1ml of isolated mitochondria at the concentration of 0.5 µg/ µl were taken in a tube and placed on ice. MT was carried out through ice cold insulin syringe in gastrocnemius (GS) muscle at 2 different sites, 3 sites in quadriceps muscle and 1 site in tibialis anterior (TA) muscle at each with 50 µl volume. The mitochondria were taken up very carefully in syringe to avoid any damage and during MT, released very slowly to avoid mitochondrial rupture and outflow from muscle during injection.

2.8 Establishment of skeletal muscle injury models

Albino BALB/c mice at the age of 7 to 8 week whose weights ranged from 25 to 30 g were selected for skeletal muscle injury models. This age mimics young adults which correspond to developmental stage, having the ability to respond to injury in muscle regeneration and recovery process. Two models of different skeletal muscle injuries were generated including Dexamethasone-induced skeletal muscle atrophy and BaCl₂-induced skeletal muscle injury model.

2.9 Dexamethasone-induced muscle atrophy mice model

In case of dexamethasone (dexa)-induced muscle atrophy mice model, all male mice were selected because dexa is a synthetic glucocorticoid steroid which can yield varying effects in male and female mice (M. J. Kim *et al.*, 2023). Mice were distributed to 6 groups including sham, vehicle control (VC), dexa-20mg/Kg (dexa-high), dexa-5mg/Kg (dexa-low), and dexa-low dose+mito. Dexa low and high doses concentrations (in mL), 5mg/Kg of mice weight and 20mg/Kg of mice weight were calculated using following dosing formula.

The experiments were designed for a total of two weeks (14 days) where dexa was administered interperitoneally (IP) once a day for seven days consecutively to dexa high, dexa-low and dexa-low+mito groups respectively, (**Fig. 2.3**).

$$= \frac{\text{Required dose (mg/Kg)} \times \text{body weight (Kg)}}{\text{Stock (mg/ml)}}$$

Normal saline was administered IP to VC group mice. MT was carried out locally in mice hind limb gastrocnemius (GS), tibialis anterior (TA) and quadriceps (QD) skeletal muscles of dexa+mito groups at 7th day of dexa IP

injections. Body weights of all mice were consecutively measured at each third day for two weeks.

At the 15th day of experiment all mice were sacrificed, (**Fig. 2.3**) after anesthetizing with chloroform. Blood was safely drawn from the heart of each mouse and carefully released to a 1.5 ml microcentrifuge tubes without haemolysis in order to correctly measure serum levels of LDH. GS and TA muscles of hind limbs were removed, weighed, and immediately added to the tubes containing normal saline placed on ice. Sections of GS muscles were saved in 10% formalin for histological processing and haematoxylin and eosin (H/E) staining.

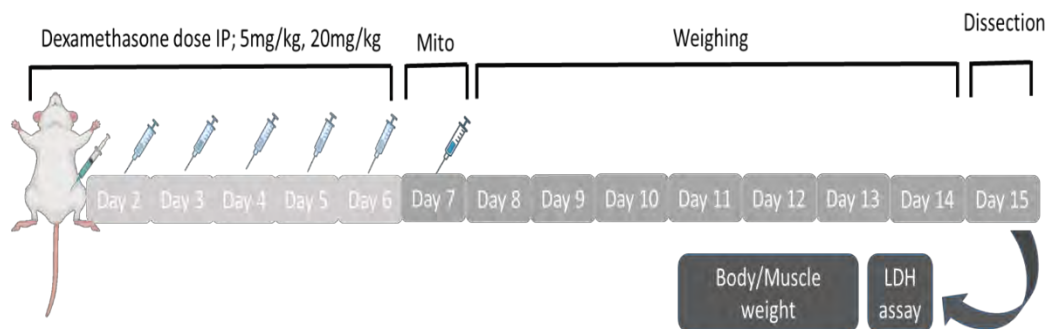


Fig. 2.3 *Experimental plan for dexamethasone-induced skeletal muscle atrophy model generation.*

2.10 Barium chloride (BaCl₂)-induced skeletal muscle injury mice model

In BaCl₂-induced muscle injury experiment, male and female mice were randomly selected. Both male and female selection is important for understanding of intricate interplay of cellular and molecular process both sexes happening during muscle injury. The protocol was in accordance with the previous reports (A. B. Morton *et al.*, 2019). Three groups were selected including VC, BaCl₂-alone, and BaCl₂-mito. The hind limbs were shaved with hair removal cream. 1.2 % of BaCl₂ were prepared and then 50 µl from it were injected locally in GS muscles to induce myotoxic injury in BaCl₂-alone and BaCl₂ +mito groups. Normal saline was injected in GS muscles of VC group. Viable isolated mitochondria (0.5 µg/µl) were then transplanted locally into the injured GS muscles of BaCl₂ +mito group 24 hours post injury. The mice were sacrificed 24 hours after the MT, (**Fig. 2.4**). Blood was drawn from mice hearts

carefully for muscle injury marker analysis in serum (LDH). GS muscles from all mice groups were removed and weighed. Then, a section from each GS muscle were stored in 10% formalin for histological analysis, H/E staining, while the other section of GS muscle was saved for muscle infarct size analysis using TTC staining assay.



Fig. 2.4 *Experimental design of BaCl₂-induced muscle injury model*

2.11 TTC staining assay

The sections of GS muscles were taken to find the infarct area by using 2,3,5-triphenyltetrazolium chloride (TTC) assay. During the muscle isolation, the fatty and connective tissues layers (epimysium) were carefully removed. Small pieces were cut transversely and placed in 1 % TTC for 1 hour at 37°C in dark. TTC is a colourless salt that is soluble in water and sensitive to light. An enzyme called succinate dehydrogenase present in mitochondria of viable tissues, converts TTC into formazan and stains the healthy tissues as deep red that, the necrotic tissues as pale yellow while the connective tissues remain white. Although the colour of skeletal muscles vary from individual to individual but mostly look reddish-pink due to presence of myoglobin. The tissue sections were dried at filter paper and then observed under a stereomicroscope (**Fig. 2.5**). The infarct zone was calculated by the ratio of area of necrotic region (NR) to the area at risk (AAR). The images taken were analysed by Image J software (NIH, USA) and the relative infarct size were quantified through dividing the NR by the AAR, using following formula.

$$\text{Necrotic size} = \text{necrotic region} / \text{Area at risk}$$

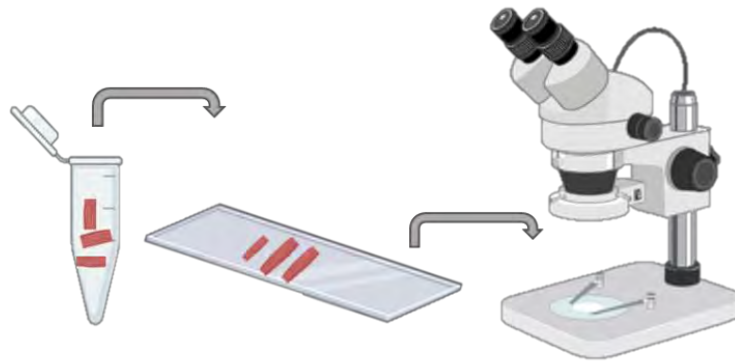


Fig. 2.5 TTC staining and observation under stereomicroscope. *GS muscle transverse section placed in 400 μ l of 1 % TTC for 1 hr at 37°C, transferred to slide and observed under microscope (made by Biorender.com).*

2.12 Lactate dehydrogenase (LDH) assay

The blood was preserved carefully from mice through cardiac puncture, then proceeded for serum isolation and centrifuged at 2000 x g for 15 minutes. The substrate solution of LDH assay kit containing lactate and NAD was prepared, (**Fig. 2.6**). The temperature of serum and LDH solution was pre-raised in incubator for their optimal activity during the reaction. Spectrophotometer “Multiskan Go” (Thermo Fisher Scientific, USA) was also set at 37°C. The absorbance of LDH reaction with its substrate was recorded at 340nm. The cuvette was first air blanked to avoid background absorbance, calibrate the instrument and set the base line for correct absorbance. Next, 500 μ l of LDH substrate solution was added and reading was taken then, 10 μ l of serum were poured and immediately the reading was taken, further two readings were collected with the interval of 1 minute. To find the serum LDH level, delta absorbance was calculated by subtracting each value from the subsequent value. The average of two values were calculated and multiplied with 8095 and the result was presented as LDH (U/L).

2.13 Histological analysis

Sections of GS muscles of dexamethasone-induced muscle atrophy model were saved in 10% formalin at room temperature. Tissue was processed and sections were stained with haematoxylin and eosin (H/E) stain followed by mounting. The slides were observed under a brightfield microscope (OPTIKAB5, Digital

camera 4083.B5, Italy) and images were taken through mobile phone camera. H/E staining is used for histological analysis where in haematoxylin stains the nucleus in blue and eosin an acidic dye stained the cytoplasm and extracellular matrix in pink. The cross-sectional area (CSA) of muscle fibers was calculated by image j software (NIH, USA).

2.14 Statistical analysis

For body and muscle weight, LDH, TTC, CSA, statistical analysis of data was performed by Graphpad-prism 5 (Graphpad Software, San Diego, CA, USA). One way ANOVA with Bonferroni's post-test was applied for comparison of three groups and the T-test applied for comparison of two groups. Data prior to statistical tests were proceeded and normalized by Microsoft Excel software.

3. Results

Dexamethasone causes skeletal muscle atrophy in mice

Dexamethasone (dexa) is a synthetic glucocorticoid that is commonly used as anti-inflammatory and immunosuppressant drug in clinical practices (Hodgens *et al.* , 2022). The prolonged exposure to dexa high dose (dexa 20mg/kg) is correlated with muscle atrophy and is characterized by imbalance in protein synthesis and degradation and therefore result in retarded myogenesis (Ozaki *et al.* , 2023).

3.1 High dose of dexa (20mg/kg) induced severe physical impairment

The intraperitoneal (IP) administration of dexa (20mg/kg) for 15 consecutive days revealed weakened mice bodies, poor fur quality and apparent decrease in body volume compared to vehicle control (VC) group. The morphology of dexa (20mg/kg) group revealed curved back bone due to muscle weakness and restricted locomotion, (**Fig. 3.1**).

3.1.1 Dexa (20mg/kg) reduced mice body weight

Although dexa is used as anti-inflammatory and immunosuppressant, however high doses have negative effects also. The IP administration of high concentration of dexa (20mg/kg) has been found to reduce the body weight as a whole (Yoshikawa *et al.* , 2021). The body weight data obtained at every third day showed that high dose of dexa (20mg/kg) resulted in a significant decline in body weight compared to VC mice (**Fig. 3.2 A**). The net change in body weight of dexa-treated mice is also significantly lower than that of the respective control, (**Fig. 3.2 B**).

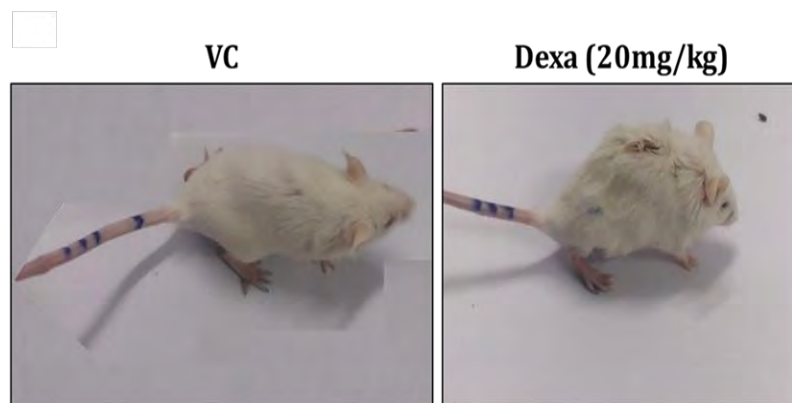


Fig. 3.1 The physical features of mice with dexa high dose (20mg/kg). *The bodies of mice were very weak with limited locomotion, low body volume and poor fur quality following dexa implementation dexa mice compared to VC mice.*

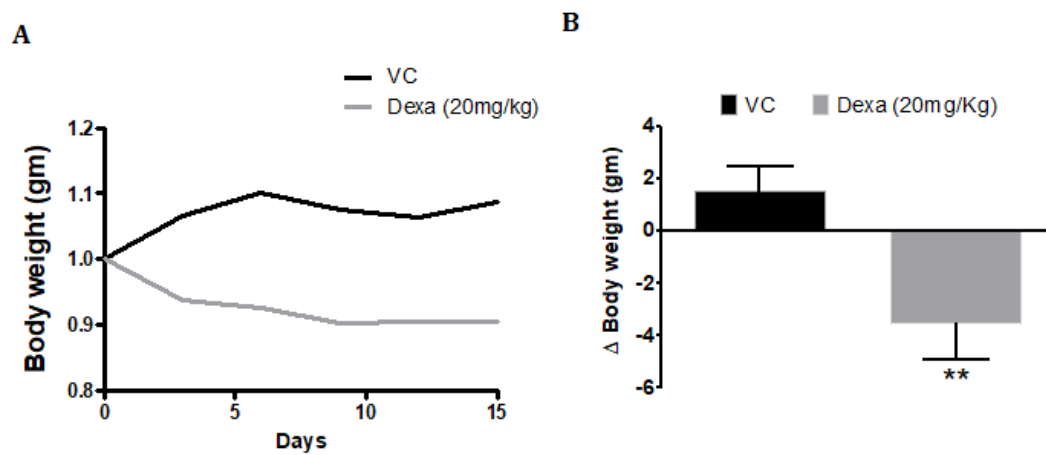


Fig. 3.2 Loss of body weight in mice administered with high dose of dexamethasone. **A)** The net body weight in dexamethasone (20mg/kg) mice compared to VC mice for 15 days of measurement. **B)** The mean change in weight between day 1 and day 15 of the experiment represented as mean \pm SEM, $n=6$, $**p<0.01$

3.1.2 High dose of dexamethasone caused a reduction in individual muscle's weight

We carefully isolated three muscles of hind limb including gastrocnemius (GS), Tibialis anterior (TA), and quadriceps (QD). The weight of both VC and dexamethasone muscles was measured that showed a variable change in the weight in different muscles. In GS muscles there was no difference in (**Fig. 3.3 A**) while in TA muscles there was a little tendency towards reduced muscle mass, (**Fig. 3.3 B**) But, interestingly, in case of QD muscles there was an increased tendency towards a reduced muscle weight (**Fig. 3.3 C**).

3.1.3 Dexamethasone (20mg/kg) reduced muscle fiber cross sectional area (CSA)

Microscopic observations of skeletal muscle cross sections predicted several changes in dexamethasone-treated muscles. These examinations included the composition, muscle activity and tissue health (Seo *et al.* , 2022). After assessment of dexamethasone high dose impact on body weight we performed the histological examination of GS muscles to find its influence at cellular level. Microscopic analysis of H&E-stained tissues sections of GS muscles of VC and dexamethasone (20mg/kg) groups revealed an apparent reduce in muscle fiber CSA in dexamethasone (20mg/kg) group compared to VC group (**Fig. 3.4 A**). Similarly, examination of tissue sections of GS muscle also revealed apparent increase in endomysium spaces between muscle fiber bundles in dexamethasone (20mg/kg) compared to VC group, as shown in **Fig. 3.4 A**. Next the analysis of CSA data obtained through image J revealed a significant decline in muscle fiber CSA dexamethasone (20mg/kg) mice compared to VC mice (**Fig. 3.4 B**).

3.1.4 Dexamethasone (20 mg/kg) treatment upraised serum LDH levels

Lactate dehydrogenase (LDH) is responsible for the reversible conversion of pyruvate to dehydrogenase in many tissues including skeletal muscles (Farhana *et al.* , 2020). LDH is leaked out to blood stream whenever there is a damage to skeletal muscle cell membrane (Ali *et al.* , 2021). Thus, LDH was used as a muscle injury marker in the blood. The data revealed a non-significant increase in LDH level in dexamethasone (20mg/kg) group compared to the VC group, (**Fig. 3.5**)

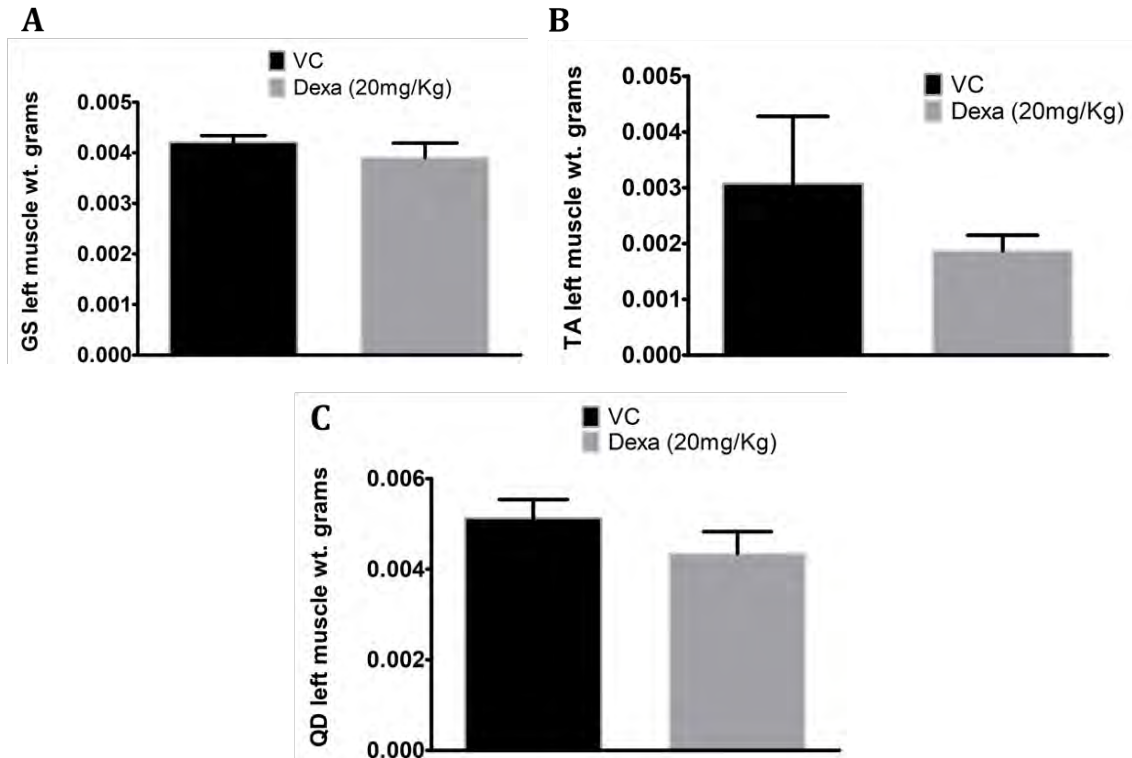


Fig. 3.3 Change in muscle mass of dexamethasone-treated mice. *A)* Represents GS muscle weight of dexamethasone (20mg/kg) compared to VC. *B)* Denotes QD muscles of dexamethasone (20mg/kg) compared to VC and, *C)* shows TA muscles mean change in Dexamethasone (20mg/kg) compared to VC. The values of all muscle masses were normalized with their respective mice body weights and represented as mean \pm SEM. $n=6$, GS; Gastrocnemius, QD; Quadriceps, TA; Tibialis anterior.

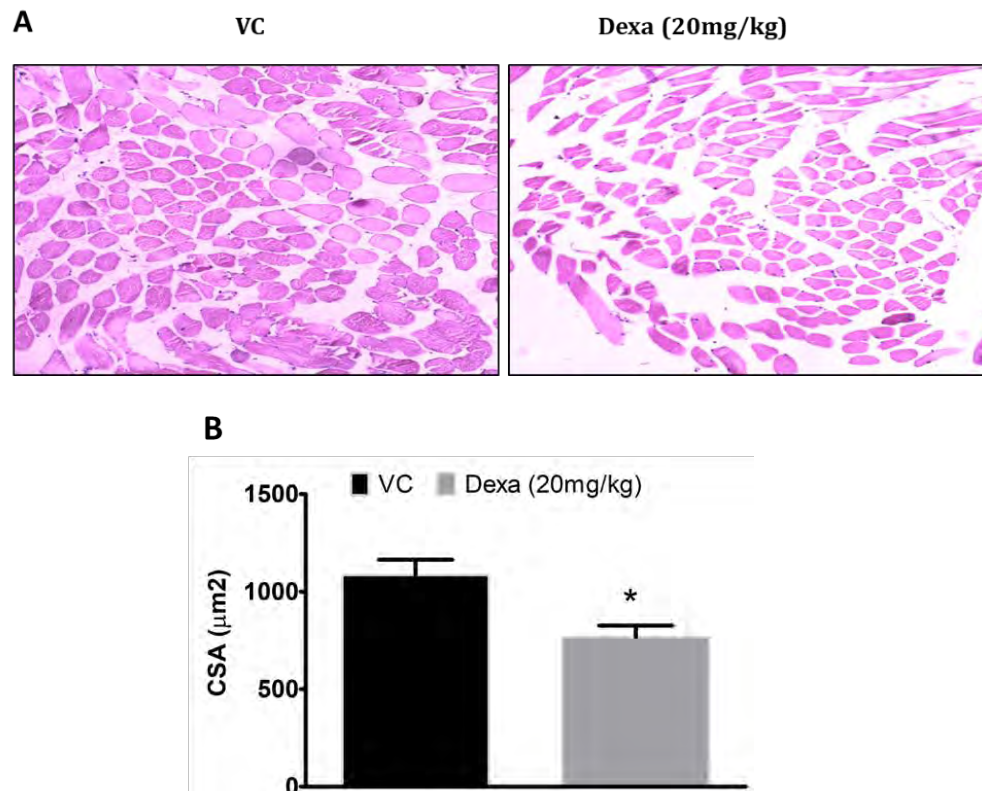


Fig. 3.4 Reduced muscle fiber cross section area in dexa treated mice. A) The cross sections of H&E-stained GS (gastrocnemius) muscles demonstrate change in muscle fiber cross sectional area (CSA) and endomysium space size in dexa (20mg/kg) mice compared to VC mice. **B)** Mean change in muscle fiber CSA of GS muscles in dexa (20mg/kg) mice compared to VC represented as , * $p < 0.05$.

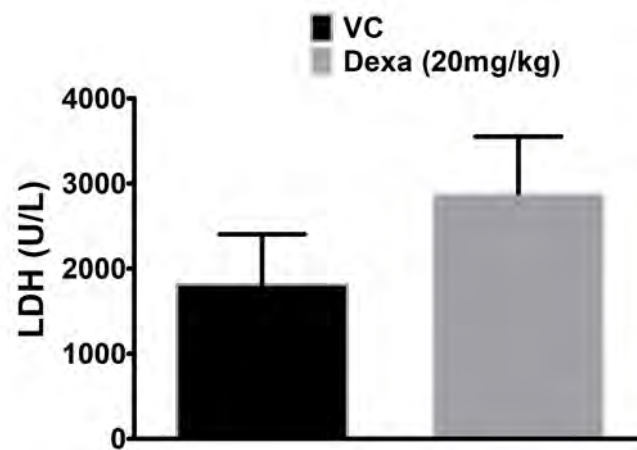


Fig. 3.5 The observable increase in serum LDH level in dexa-treated mice. The graph shows serum LDH levels in dexa (20mg/kg) mice compared to VC mice. The data obtained from the subsequent subtraction and mean of absorbance values taken through spectrophotometer per minute and multiplied by 8095, as $U/L = \Delta A / \text{min} * 8095$.

3.2. Low dose of dexamethasone (5mg/kg) induced muscle atrophy

The introduction of high dose of dexamethasone (20mg/kg) resulted in a significant reduction in body weight and we found that there was a high injury rate and mortality rate. We hypothesized that this may have happened due to impaired wound healing (Argilés *et al.*, 2016). Then, we decided to use a low dose dexamethasone (5mg/kg) to develop muscle atrophy model.

The IP administration of low dose of dexamethasone (5mg/kg) resulted in reduced body weight which was evident from both real-time and net change in body weight (**Fig. 3.6 A & B**). Besides the body weight, the evaluation of dexamethasone low dose (5mg/kg) effects on the hindlimb muscle mass and volume exhibited that there was some observable effect on TA and QD muscles while no effect was observed on GS muscle (**Fig. 3.7 A, B & C**). The development of the dexamethasone low-dose (5mg/kg)-mediated muscle atrophy was then evaluated by measuring LDH levels in the serum. We found an increased serum LDH levels following the treatment of low dose of dexamethasone (**fig. 3.8**).

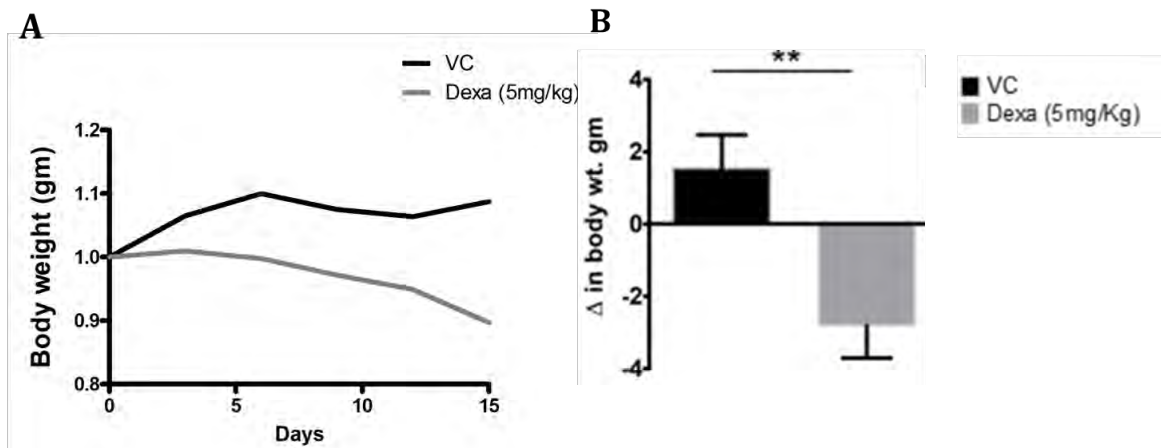


Fig. 3.6 Low dose of dexamethasone caused reduction in body weight. **A)** Day wise change in body weight of mice treated with dexamethasone low dose (5mg/kg) compared to VC mice for 15 days of measurement. **B)** Represents the net change in body weight in dexamethasone treated mice compared to VC mice. Data presented as mean \pm SEM, where $n=3$.

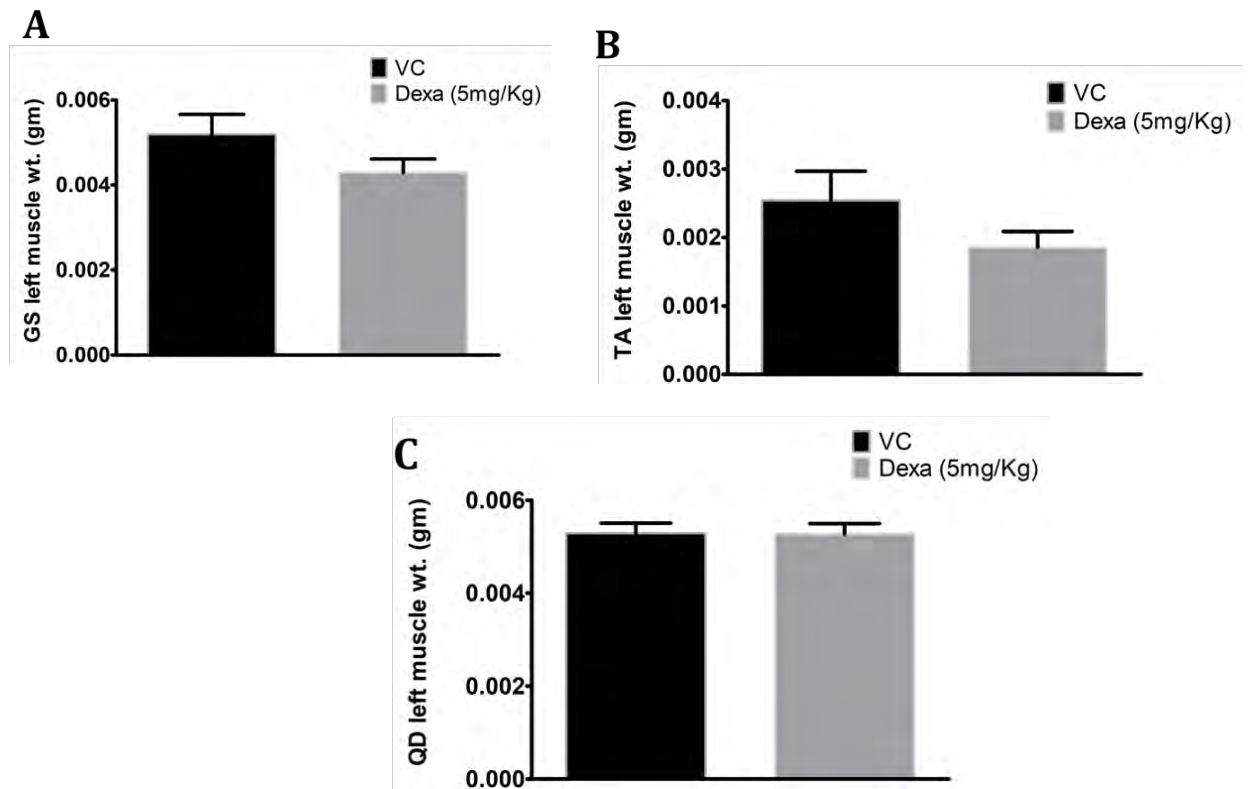


Fig. 3.7 Change in muscle mass due to low dose of dexamethasone. **A)** Represents GS muscle weight of dexamethasone (5mg/kg) compared to VC. **B)** Denotes QD muscles of dexamethasone (5mg/kg) compared to VC and, **C)** Represents mean change in dexamethasone (5mg/kg TA muscle compared to VC muscle. The values of all muscle masses were normalized with their respective mice body weights and represented as mean \pm sSEM n=5 GS; Gastrocnemius, QD; Quadriceps, TA; Tibialis anterior

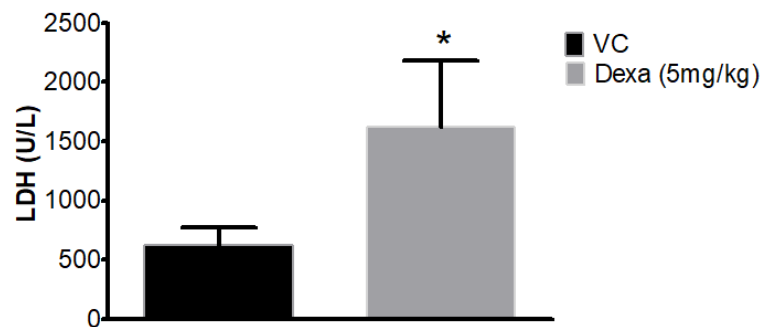


Fig. 3.8 Low dose of dexa caused an increase in serum LDH levels. *The graph shows serum LDH levels in dexa (5mg/kg) mice compared to VC mice, n=5, *p<0.05.*

3.3 Comparative effects of low (5mg/kg) and high dose (20mg/kg) dexamethasone on body weight and serum LDH levels

The relative effect of high and low doses of dexamethasone was evaluated by comparing change in body weight and serum level. There was no significant difference between high and low dose (**Fig. 3.9 A**). Similarly the investigation of relative serum LDH levels revealed that dexamethasone (20mg/kg) mice were showing an increasing trend in LDH level relative to dexamethasone (5mg/kg) mice as shown in **Fig. 3.9 B**. Based on these results, and keeping the dose safety on animal survival, we proceeded with the low dose dexamethasone rather than high dose for the investigation of the therapeutic effect of mitochondrial transplantation.

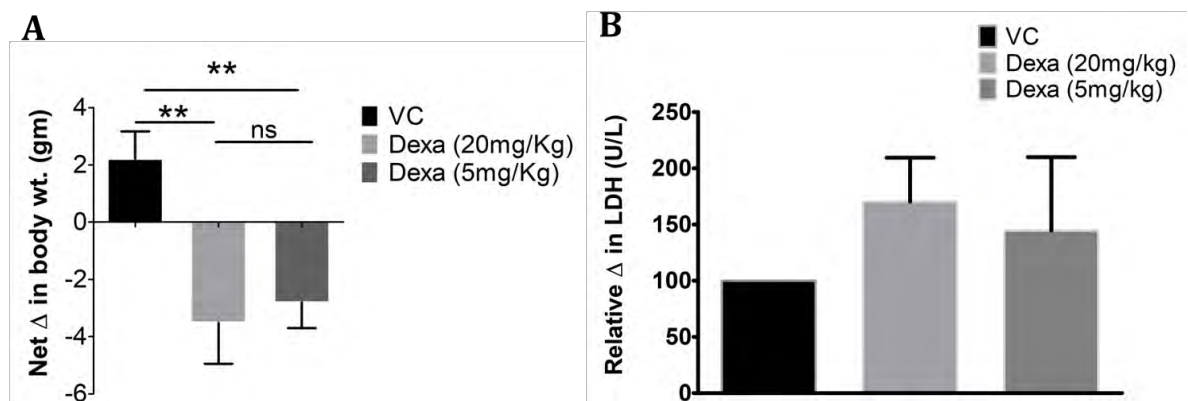


Fig. 3.9 Dexa high and low doses have differentially reduced body weight and serum LDH levels. **A)** Represents the net change in mice body weight in dexa high dose (20mg/kg) and low dose (5mg/kg) mice compared to VC mice. The mean of body weight of 6 mice presented as mean \pm SEM, * p < 0.01. **B)** Serum LDH levels in dexa (20mg/kg) and dexa (5mg/kg) mice measured in comparison to VC mice. The data is presented as mean \pm SEM, n = 6.

3.4 BaCl₂-induced skeletal muscle injury

BaCl₂ is a chemical that can induce myotoxic injuries through muscle fiber plasma membrane disruption and actomyosin proteolysis. We used this chemical to induce skeletal muscle injuries in mice in order to study the regeneration process following MT. After the administration of BaCl₂ locally in hind-limb muscles of mice, we performed the gross examination of muscle morphology. It revealed that 24 hours after the injury in hind-limb muscles appeared to have a peaked hemorrhagic edema with reddish colouration compared to pinkish pale colour of VC hind-limb muscles. (**Fig. 3.10**).

3.4.1 BaCl₂- induced muscle necrosis

We preserved GS muscles and then performed TTC staining assay. This assay stains non necrotic muscle as deep red and necrotic or dead tissue as pale yellow (C. Liu *et al.* , 2019). We carried out TTC staining of gastrocnemius (GS) muscles and then calculated the ratio of necrotic to non-necrotic zone. The data revealed that BaCl₂ increased the necrosis with more pale-yellow colour as compared to VC group which was more reddish in colour (**Fig. 3.11 A**). When the necrotic and non-necrotic area were measured through image J software, we obtained significant difference with large necrotic area in BaCl₂-treated muscles as compared to VC group (**Fig. 3.11 B**).

3.4.2 Serum LDH level in BaCl₂-induced muscle injury

The BaCl₂-mediated muscle necrosis is known to burst out LDH to systemic circulation which can be used as skeletal muscle injury index (C. Liu *et al.*, 2019). We performed the measurement of serum LDH to assess the muscle injures. The data revealed that there was increasing trend in serum LDH level in BaCl₂ group compared to VC group as shown in **Fig. 3.12**.

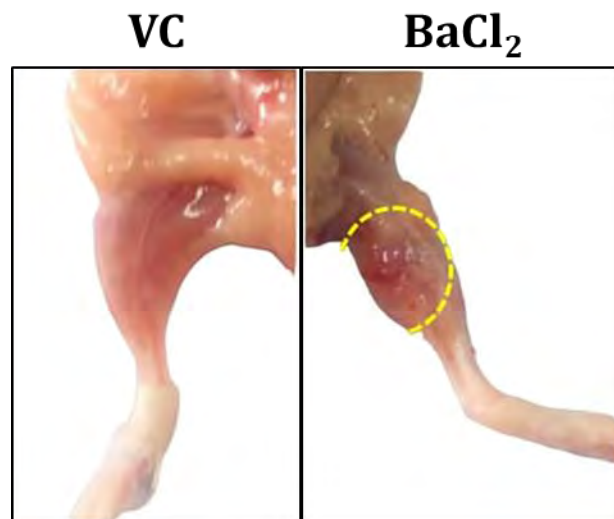


Fig. 3.10 BaCl₂ induced muscle injury in hind-limb muscles. Shows the effect of 1.2 % BaCl₂ administration in GS muscles compared to non-exposed GS muscles. GS: Gastrocnemius.

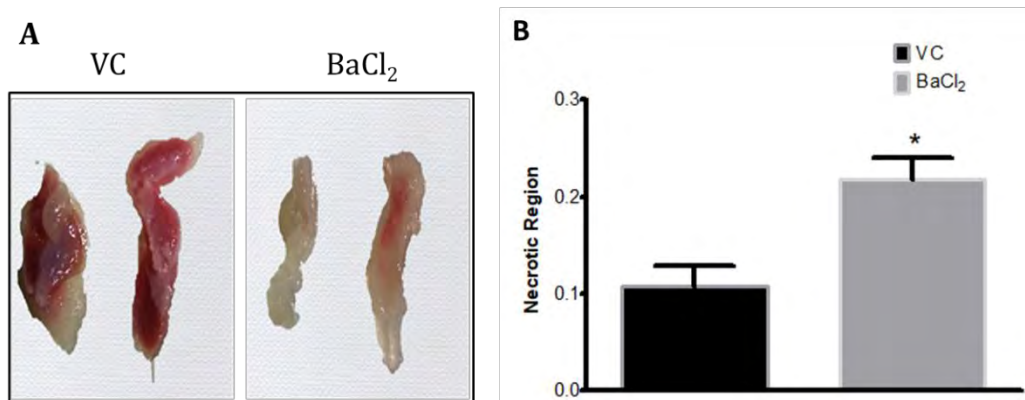


Fig. 3.11 BaCl₂-induced necrosis in GS muscle. *A)* Shows muscle necrosis in BaCl₂ treated GS muscle sections compared to non-treated GS muscles. The BaCl₂ treated muscles with pale yellow colour compared to VC muscles with deep red colour. **B)** The graphical representation of muscle necrotic size in BaCl₂ treated mice compared to VC mice. The data is revealed as mean±SEM, ($p=0.011$), of necrotic size of BaCl₂ treated mice compared to VC muscles.

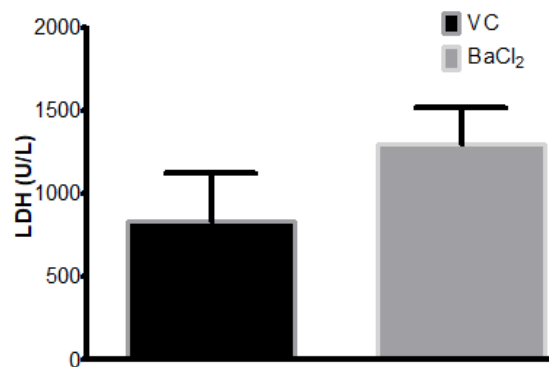


Fig. 3.12 Increased serum LDH level in BaCl₂ treated mice. *Serum LDH level in BaCl₂ treated mice compared to VC mice. The data of serum LDH level was obtained from the recorded absorbance values at 340 nm and further analyzed as $U/L = \Delta A / \text{min} * 8095$. The final data was plotted on the graph as mean \pm SEM.*

3.5 Isolated mitochondria demonstrated respiration competency and viability

Oxygen is known to be mainly consumed in the process of oxidative phosphorylation (OXPHOS). On this basis oxygen consumption rate (OCR) in a closed chamber is considered as an important functional assay for mitochondrial functional assessment. Rate of change in chamber's oxygen level is a determinant of mitochondrial health, the more the reduction, the healthier the mitochondria. According to our data mitochondria isolated with differential centrifugation technique were found viable and healthy, as evident from the higher amplitude compared to assay buffer (AB) (**Fig. 3.13 A&B**).

MTT (3-(4,5-dimethylthiazol-2-yl)-2,5-diphenyltetrazolium bromide) assay is another assay used to assess the viability of isolated mitochondria. MTT is a water insoluble yellow color tetrazolium salt which is converted to purple formazan crystals by mitochondrial resident dehydrogenases. The extent of formazan crystallization is directly proportional to the extent of mitochondrial metabolic activity. The increase absorbance values revealed that isolated mitochondria were metabolically active as shown in **Fig. 3.13 C**.

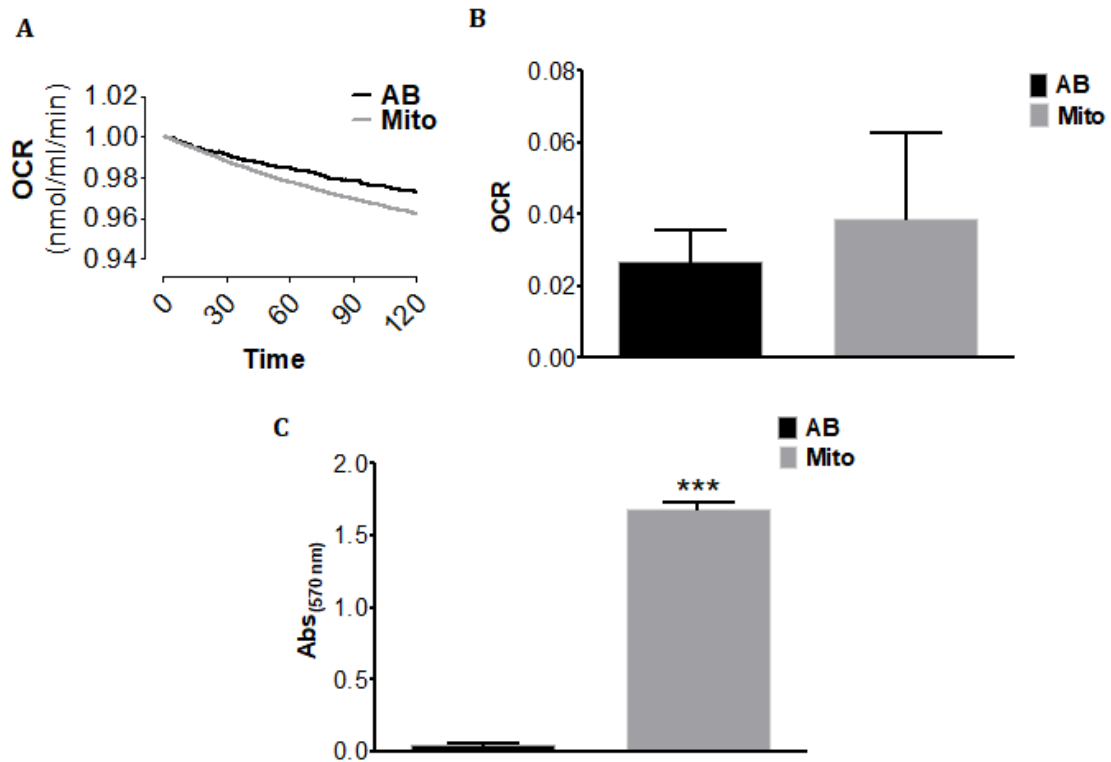


Fig. 3.13 Functional assessment of isolated mitochondria *A*) Real-time mitochondrial oxygen consumption rate (OCR) of isolated mitochondria compared to assay buffer (AB), $n=2$. *B*) Extent of OCR in isolated mitochondria compared to AB. *C*) Absorbance value of formazan crystals of isolated mitochondria compared to AB, $n=3$, $***p<0.001$.

3.6 Mitochondrial transfer (MT) recovered the body weight loss in dexamethasone-treated mice

Local MT in hindlimb muscles of GS, TA and QD were performed. The mice body weight was recorded each day for 15 days of experiment. The data of body weights measured at 3-day intervals during the whole experiment, revealed that dexamethasone significantly reduced the net body weight in dexamethasone (5mg/kg) mice compared to vehicle control mice while MT significantly increased the body weight in dexamethasone+mitochondria mice compared to vehicle control mice, (**Fig. 3.14 A**). Similarly, the data of mean change in body weight during experimental periods also exhibited that the body weight of dexamethasone (5mg/kg) mice was significantly reduced compared to vehicle control mice and the MT significantly rescued the body weight in dexamethasone+mitochondria mice compared to vehicle control mice, (**Fig. 3.14 B**).

3.7 MT and muscles mass in Dexamethasone-treated Mice

In order to further dissect the impact of exogenous healthy liver mitochondria, MT was carried out into the hind-limb muscle of dexamethasone-treated mice to assess its impact on the mass of individual muscle weight. MT in GS, TA and QD muscles revealed that there was no apparent change in muscle weight in case of MT transfer into GS muscles of dexamethasone-treated mice as compared to dexamethasone group (**Fig. 3.15 A**). However, in case of TA muscle, the data revealed that MT showed a trend in muscle weight gain in dexamethasone+mitochondria group compared to dexamethasone (5mg/kg) group (**Fig. 3.15 B**). In case of QD muscles, there was a decreasing trend in dexamethasone+mitochondria group compared to dexamethasone (5mg/kg) group (**Fig. 3.15 C**).

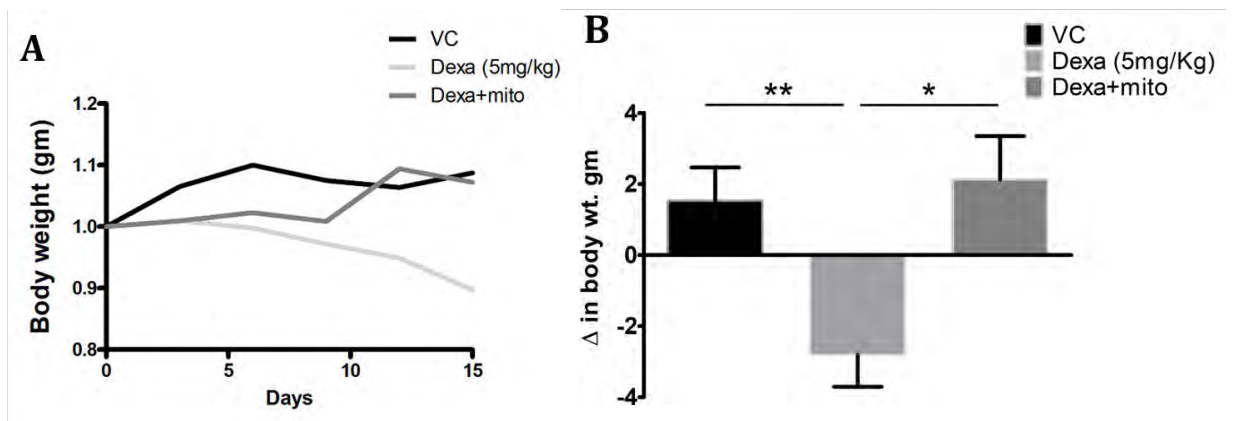


Fig. 3.14 Mitochondrial transplantation alleviated body weight loss. **A)** *The net change in body weight in dexa (5mg/kg) mice compared to VC group, and dexa+mito mice compared to VC and dexa (5mg/kg) mice. The body weight measured for 15 days was presented as mean±SEM of 6 mice in each group, ** $p < 0.01$.* **B)** *The mean weight change in mice was measured as the difference of day 1 and day 15 of experiment, and data presented as bar graph demonstrating mean (mean±SEM) weight difference in dexa+mito mice following MT compared to dexa (5mg/kg) and VC mice, ** $p < 0.01$ MT: Mitochondrial transplantation.*

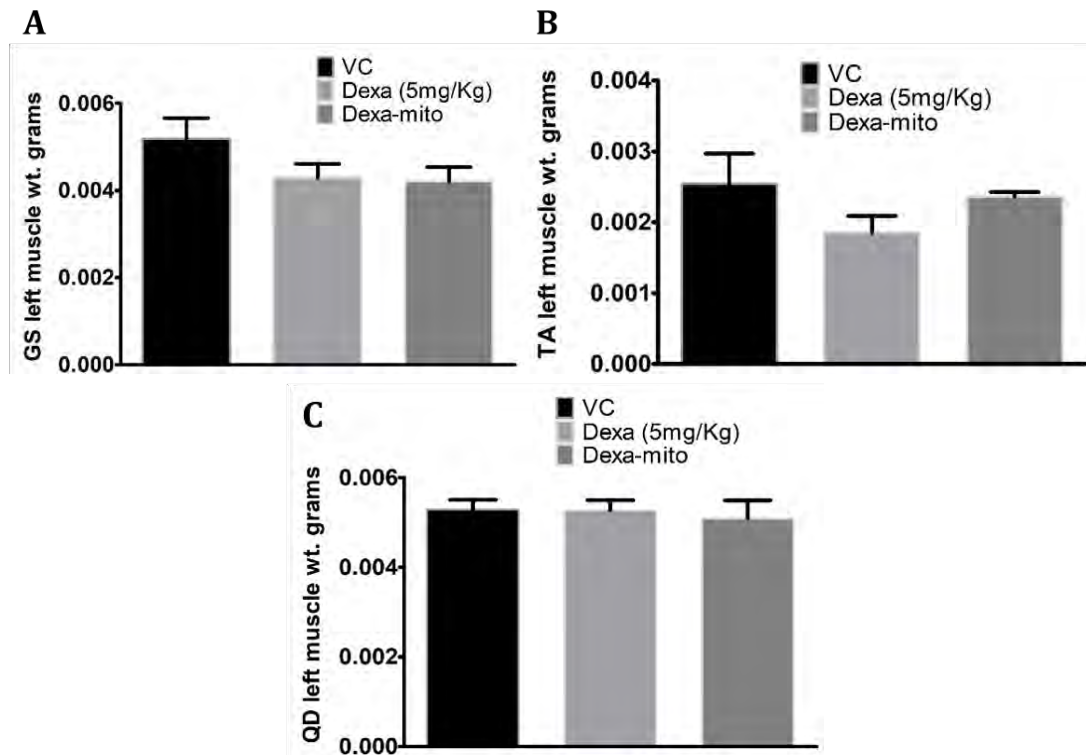


Fig. 3.15 MT resulted in no change in individual muscle weight in dexa-treated mice. **A)** Represents GS muscles weight (normalised with their respective mice body weight) in dexa+mito mice compared to dexa (5m/kg) and VC mice. While **B)** indicates weight of TA muscle (normalised with their respective mice body weight) in dexa+mito mice compared to dexa (5m/kg) and VC mice. **C)** The mean QD muscle weight in dexa+mito mice compared to dexa (5m/kg) and VC mice normalised with respective mice body weight. GS; Gastrocnemius, TA; Tebialis anterior, QD; Quadriceps.

3.8 Impact of MT on Muscle Volume

Dexa-induced muscle atrophy is characterized by loss in muscles weight and volume. The reduction in muscle volume decreases muscle strength and activity, thus leading to poor mobility and so physical performance (X. Wang *et al.* , 2013). We aimed to find the effect of MT on individual muscle volume. For this purpose, we used common formula of volume (Length*Width*Height) and then normalised the values of individual muscle volumes with their relevant muscle mass. The data analysis revealed that there was no change in dexa+mito group compared to dexa (5mg/kg) in all three muscles including GS, TA and QD, as shown in **Fig. 3.16**.

3.9 MT affected serum LDH level

To further investigate the impact of MT on dexa-treated mice we measured the serum LDH as muscle injury marker. The analysis of data revealed that mice treated with MT showed a non-significant decrease in serum LDH level compared to dexa (5mg/kg) as shown in **Fig. 3.17**.

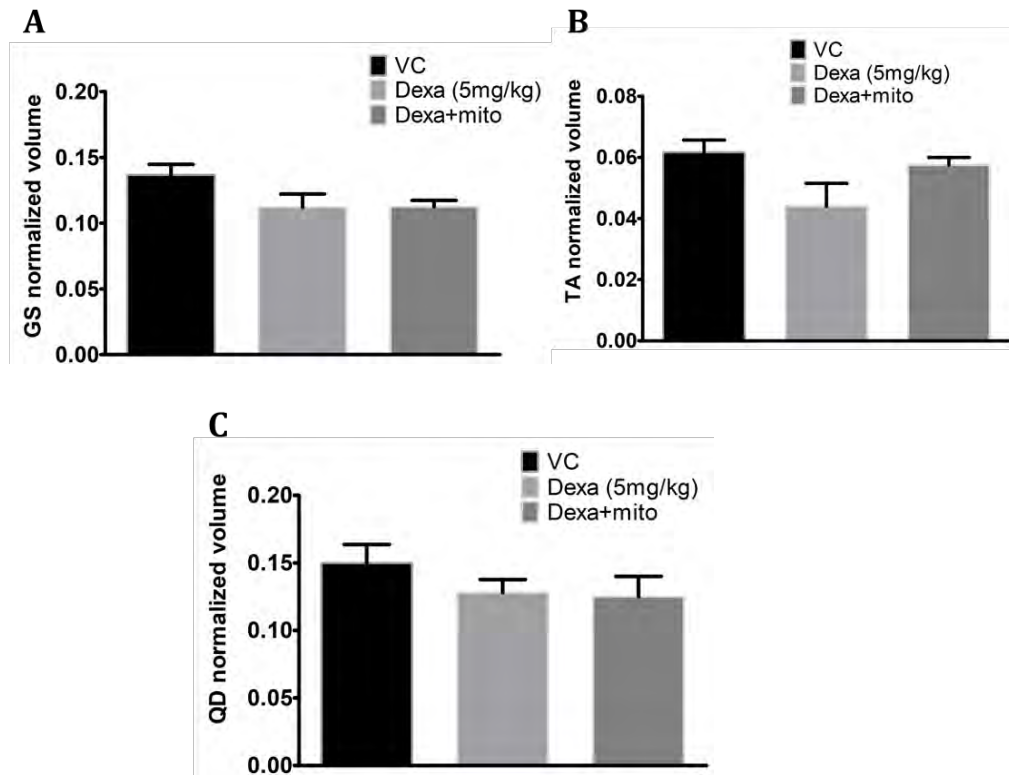


Fig. 3.16 Mitochondrial transplantation and muscle volume. *A)* The presentation of normalised GS muscle volume in dexa+mito mice compared to dexa (5mg/kg) and VC mice analysed as of 6 mice muscles. *B)* Represents the MT in TA of dexa+mito mice and its normalised volume compared to dexa (5mg/kg) and VC mice, mean \pm SEM of 6 mice muscle in each group. *C)* Shows the mean volume in QD of dexa+mito mice after MT compared to dexa (5mg/kg) and VC mice. GS; Gastrocnemius, TA; Tibialis anterior, QD; Quadriceps.

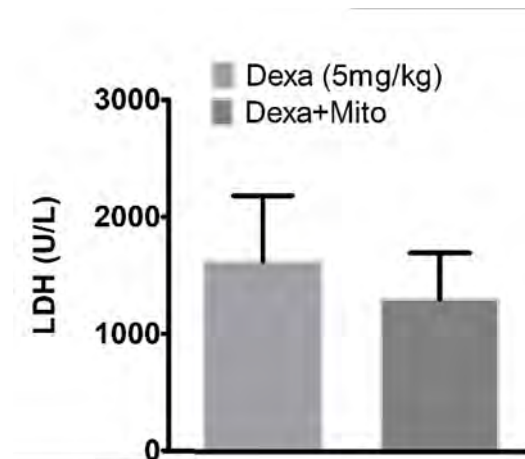


Fig. 3.17 Serum LDH release was decreased upon MT. *The graph shows serum LDH levels in dexa+mito after MT mice compared to dexa (5mg/kg).*

3.10 MT demonstrated positive effect on muscle weight gain in BaCl₂-treated mice

Mitochondria is known to have an important role in muscle regeneration and repair following injury. With this background, we performed MT in GS muscles locally and it revealed that GS muscles of BaCl₂+mito group showed a positive but non-significant increase in muscle weight gain compared to BaCl₂ group as shown in **Fig. 3.18**.

3.11 MT exhibited no change in serum LDH level

The existing literature highlights that the LDH level reduces when muscle recover from injury (Jiaming *et al.* , 2021). We also employed LDH level to evaluate the impact of MT on muscle induced by BaCl₂. Our data revealed that MT has not recovered the increased LDH release, (**Fig. 3.19**)

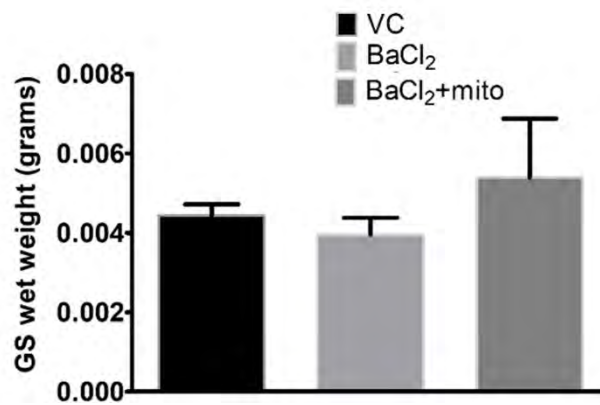


Fig. 3.18 MT demonstrated increased trend in muscle mass of BaCl₂ treated mice. The mean weight of GS muscle in BaCl₂+mito mice following MT compared to VC and BaCl₂ treated mice represented as mean \pm SEM.

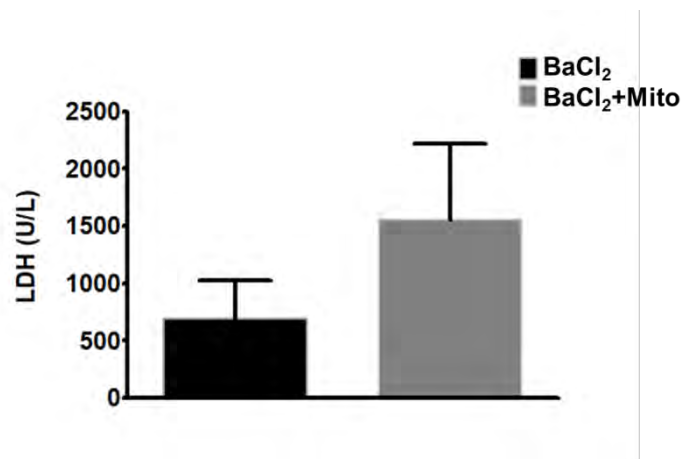


Figure. 3.19 MT revealed no impact on LDH level. *The graph shows serum LDH level following MT.*

4 Discussion

Mitochondrial transplantation is an emerging technique that has shown promising results in mitochondrial myopathies (Park *et al.* , 2021), neurologic disorders (Huang *et al.* , 2016), diabetes (Y. Chen *et al.* , 2022), kidney diseases (Hernández-Cruz *et al.* , 2022), liver diseases (Lin *et al.* , 2013), cardiovascular (McCully *et al.*, 2009), and skeletal muscle injuries (Orfany *et al.*, 2020).

In this study we aimed to investigate (as a proof of concept) the impact of exogenous mitochondrial transplantation on dexamethasone-induced skeletal muscle atrophy and BaCl₂-induced skeletal muscle injury. Myopathies including skeletal muscle atrophy and chemicals-induced muscle injuries occur as a consequence of imbalanced protein metabolism and ionic distribution ultimately resulting in muscle weakness and loss of function. The impact of high and low dose dexamethasone (dexa) was explored followed by mitochondrial transplantation as a therapeutic strategy. Dexa is known to induce skeletal muscle atrophy, characterized by muscle wasting, and loss in muscular strength and function due to imbalance in protein turnover. Dexa causes body weakness, limited locomotion (Cid-Díaz *et al.* , 2021) and reduced motor coordination (Tieland *et al.* , 2018). We found that high dose (20mg/kg) of dexa resulted in body shrinkage, poor fur quality, reduced body weight and muscle mass, altered locomotion, myofibril degradation and increase LDH in the serum. However, high dose of dexa happened to be more lethal resulting in poor survival. Similarly, the administration of low dose dexa (5mg/kg) also resulted in lower body mass, and increased LDH level while significant effect on muscle mass. The comparative analysis of both high and low doses of dexa showed that both doses are pretty enough to induce muscle atrophy as no significant difference between the two groups. Due to the extremely deteriorating effect of high dose of dexa, we proceeded with low dexa for the rest of experiments.

Our results also showed that high dose dexa lowered the skeletal muscle fiber cross sectional area (CSA). These results are consistent with the previous studies where the quantitative measurement of CSA revealed a 47% decrease in myofibril size of the dexa-treated mice against untreated mice (Qin *et al.* , 2013). The decrease in mean diameter of skeletal muscle fibers in combination with increase in size of collagen fibers region has been demonstrated in dexa-treated

mice compared to healthy ones (J. M. Lim *et al.* , 2018). In another recent study, researcher found a significant shift toward lower CSA and small muscle fiber size upon dexamethasone administration (Seo *et al.*, 2022). This reduction in muscle fiber CSA is due to dexamethasone-mediated proteolysis, increase deposition of connective tissues, characterized by increased endomysium region, leading to muscle fibrosis and diminished muscular activity (Balboa *et al.* , 2020). Dexamethasone-elicited proteolysis is caused by elevated expression of atrogens which ultimately results in lower myofibril numbers and muscle fiber CSA (Seo *et al.*, 2022).

Skeletal muscles are heterogeneous in their nature and comprised of different muscle fiber types either glycolytic or oxidative based on metabolic programming (Jun *et al.* , 2023; Straight *et al.* , 2020). The predominance of a muscle fiber type showcases its properties. Hind limb gastrocnemius (GS) muscle are glycolytic and more prone to atrophic effect, tibialis anterior (TA) muscles are more oxidative; thus resistant to dexamethasone-mediated atrophic effect, while quadriceps (QD) muscles are composed of relatively equal number of both glycolytic and oxidative fiber types (Mukund *et al.* , 2020). In this way the response of different muscle types is distinctive towards different pathological conditions (B. Y.-H. Wang *et al.* , 2023). We found a tendency in reduced TA and QD muscle mass going in line with the literature (Seo *et al.*, 2022). Already published literature supports reduction in muscle mass upon treatment with high dose of dexamethasone (15mg/kg) (Hah *et al.* , 2022; B. Y.-H. Wang *et al.*, 2023).

Lactate dehydrogenase (LDH) is an important enzyme that catalyze the reversible conversion of pyruvate to lactate during the cellular metabolism (Farhana *et al.*, 2020). The release of LDH is an important biomarker of cellular damage and is used as a cytotoxicity index (Ku *et al.* , 2021). Our results exhibited an elevation in the serum LDH level of dexamethasone-treated mice going in line with the already published reports (J.-M. Lim *et al.* , 2019). . Dexamethasone causes damage to skeletal muscles via permeabilization of plasma membrane and therefore releases LDH to blood circulation and thus used as an indicator of altered cellular metabolic and skeletal muscle injury (Ali *et al.*, 2021; Ku *et al.*, 2021).

Healthy and bio-energetically active mitochondria are known to rescue muscle injuries besides speeding up regeneration and recovery process (S. E. Alway *et al.*, 2023). Our results of mitochondrial transplantation in dexamethasone-treated mice demonstrated an overall improvement in whole body including body mass, muscle mass and cytotoxicity index. These effects are supported by the results of umbilical cord derived mesenchymal stem cells (UC-MSCs)-based mitochondrial transfer in dexamethasone low dose treated rats which rescued the declining body weight. (M. J. Kim *et al.*, 2023). This therapeutic effect of exogenous healthy mitochondria may be exercised by elevating the metabolic rate of the recipient tissue, accelerating protein synthesis and muscle growth (Memme *et al.*, 2021). This muscle growth may contribute to overall body weight gain. Besides, our results also exhibited an increasing trend in mass gain of gastrocnemius (GS), tibialis anterior (TA) and quadriceps (QD) muscles. However, no change was observed in both GS and QD muscles following mitochondrial transfer. These results go in line with reported literature (M. J. Kim *et al.*, 2023).

We next proceeded to examine lactate dehydrogenase (LDH) as serum muscle atrophy marker, the result showed that mitochondrial transfer led towards lowering serum LDH release (Peng *et al.*, 2021). The data also demonstrated that there were no obvious changes in muscle size and volume upon mitochondrial transfer. From these findings we may predict that mitochondrial transfer exercises its effect at cellular level which may have enhanced the integrity of muscle fiber (X. Wang *et al.*, 2013).

Barium chloride (BaCl_2) is used to establish models for the investigation of muscle injuries, regeneration and for evaluating different therapeutics. BaCl_2 is preferred due to the rapid generation of injury (less time consumption) without affecting skeletal muscle stem cells (Buckingham *et al.*, 2015). Gastrocnemius muscle was selected for creating injury because it has Type IIB fibers which bear less mitochondria. Hence, making it a good candidate for experimental choice. Other types of muscles such as TA and QD are way more oxidative and already hold enough number of mitochondria. We observed hemorrhagic edema characterized by red coloration of the muscle tissue upon BaCl_2 , supported by literature where BaCl_2 application resulted in peaked hemorrhagic edema due to infiltration of red blood cells and mononuclear cells at the injury site (H.-W. Jung *et al.*, 2019). The results of muscle mass analysis showed mitochondrial transfer improved muscle mass which was previously slightly reduced by BaCl_2 as observed in a recent study of mitochondrial transfer (S. E. Alway *et al.*, 2023). The possible reason for the increase in

muscle mass after MT may be the improved healthy to non-healthy mitochondrial ratio at the injury site helping muscle stem cells to get activated, proliferate, differentiate and finally add new myotubes to injured muscle fiber (B. Kim *et al.* , 2013; Sousa-Victor *et al.* , 2016). Our results showed that BaCl₂ resulted in a non-significant increase in serum LDH levels. BaCl₂ is known to trigger membrane disruption causing leakage of LDH to blood stream (Goll *et al.*, 2003).

We studied the course of BaCl₂-induced muscle necrosis by performing TTC staining assay and found that BaCl₂ caused an increase in skeletal muscle necrosis. Unlikely, TTC staining for muscle injury is not reported, however, it has been used to study muscle injury in ischemia reperfusion injury. BaCl₂ and IRI share common pathophysiology, as both type of injuries trigger inflammation and muscle degeneration leading to necrosis or muscle infarction (H. W. Jung *et al.* , 2019; Orfany *et al.*, 2020). Interestingly, both approaches (BaCl₂ and IRI) introduce injury within 24 hours of stimulation (Jung *et al.*, 2019; Orfany *et al.*, 2020). Therefore, by relating BaCl₂ mediated injury to IRI we can validate our results and suggest that TTC may also confirm the viability and functional integrity of skeletal muscle following injury.

Conclusion

Taken together, the presented data proves that dexamethasone and BaCl₂ can be used to induce skeletal muscle atrophy and myotoxic injury respectively. Besides, the study emphasized the potential promising effects of mitochondrial transplantation as therapeutic strategy to alleviate muscle injuries. The evidence came from investigation of mice body weight and muscle mass, muscle fiber CSA, serum LDH levels and TTC staining assay. Finally, further studies are needed to improve mitochondrial isolation, purification, transfer and characterization techniques.

5. REFERENCES

- Abel, E. D. (2018). MITOCHONDRIAL DYNAMICS AND METABOLIC REGULATION IN CARDIAC AND SKELETAL MUSCLE. *Trans Am Clin Climatol Assoc*, 129, 266-278.
- Al-Menhali, A. S., et al. (2020). Lipid peroxidation is involved in calcium dependent upregulation of mitochondrial metabolism in skeletal muscle. *Biochimica et Biophysica Acta (BBA)-General Subjects*, 1864(3), 129487.
- Ali, A. M. and Kunugi, H. (2021). Skeletal muscle damage in COVID-19: a call for action. *Medicina*, 57(4), 372.
- Alway, S. E., Paez, H. G. and Pitzer, C. R. (2023). The Role of Mitochondria in Mediation of Skeletal Muscle Repair. *Muscles*, 2(2), 119-163.
- Alway, S. E., et al. (2023). Mitochondria transplant therapy improves regeneration and restoration of injured skeletal muscle. *J Cachexia Sarcopenia Muscle*, 14(1), 493-507. doi:10.1002/jcsm.13153
- Anderson, J. E. (2022). Key concepts in muscle regeneration: Muscle “cellular ecology” integrates a gestalt of cellular cross-talk, motility, and activity to remodel structure and restore function. *European journal of applied physiology*, 122(2), 273-300.
- Andreux, P. A., Houtkooper, R. H. and Auwerx, J. (2013). Pharmacological approaches to restore mitochondrial function. *Nature Reviews Drug Discovery*, 12(6), 465-483.
- Aniort, J., et al. (2019). Muscle wasting in patients with end-stage renal disease or early-stage lung cancer: common mechanisms at work. *Journal of Cachexia, Sarcopenia and Muscle*, 10(2), 323-337. doi:<https://doi.org/10.1002/jcsm.12376>
- Argilés, J. M., Campos, N., Lopez-Pedrosa, J. M., Rueda, R. and Rodriguez-Mañas, L. (2016). Skeletal Muscle Regulates Metabolism via Interorgan Crosstalk: Roles in Health and Disease. *Journal of the American Medical Directors Association*, 17(9), 789-796. doi:<https://doi.org/10.1016/j.jamda.2016.04.019>
- Balboa, E., et al. (2020). Vitamin E blocks connexin hemichannels and prevents deleterious effects of glucocorticoid treatment on skeletal muscles. *International journal of molecular sciences*, 21(11), 4094.
- Barnig, C., et al. (2022). Resolution of Inflammation after Skeletal Muscle Ischemia–Reperfusion Injury: A Focus on the Lipid Mediators Lipoxins, Resolvins, Protectins and Maresins. *Antioxidants*, 11(6), 1213.
- Beekmann, K., de Haan, L. H., Actis-Goretta, L., Houtman, R., van Bladeren, P. J. and Rietjens, I. M. (2015). The effect of glucuronidation on isoflavone induced estrogen receptor (ER) α and ER β mediated coregulator interactions. *J Steroid Biochem Mol Biol*, 154, 245-253. doi:10.1016/j.jsbmb.2015.09.002
- Bloemberg, D. and Quadrilatero, J. (2012). Rapid determination of myosin heavy chain expression in rat, mouse, and human skeletal muscle using multicolor immunofluorescence analysis. *PLoS One*, 7(4), e35273. doi:10.1371/journal.pone.0035273
- Bodine, S. C., et al. (2001). Identification of Ubiquitin Ligases Required for Skeletal Muscle Atrophy. *Science*, 294(5547), 1704-1708.
- Bottinelli, R., Pellegrino, M., Canepari, M., Rossi, R. and Reggiani, C. (1999). Specific contributions of various muscle fibre types to human muscle performance: an in vitro study. *Journal of Electromyography and Kinesiology*, 9(2), 87-95.

- Bravo-Sagua, R., Parra, V., López-Crisosto, C., Díaz, P., Quest, A. and Lavandero, S. (2017). Calcium transport and signaling in mitochondria. *Compr Physiol*, 7(2), 623-634.
- Buckingham, M. and Relaix, F. (2015). *PAX3 and PAX7 as upstream regulators of myogenesis*. Paper presented at the Seminars in cell & developmental biology.
- Cabrera, F., et al. (2019). Primary allogeneic mitochondrial mix (PAMM) transfer/transplant by MitoCeption to address damage in PBMCs caused by ultraviolet radiation. *BMC biotechnology*, 19, 1-14.
- Caicedo, A., et al. (2015). MitoCeption as a new tool to assess the effects of mesenchymal stem/stromal cell mitochondria on cancer cell metabolism and function. *Scientific reports*, 5(1), 9073.
- Call, J. A., Wilson, R. J., Laker, R. C., Zhang, M., Kundu, M. and Yan, Z. (2017). Ulk1-mediated autophagy plays an essential role in mitochondrial remodeling and functional regeneration of skeletal muscle. *American Journal of Physiology-Cell Physiology*, 312(6), C724-C732.
- Castets, P., et al. (2013). Sustained activation of mTORC1 in skeletal muscle inhibits constitutive and starvation-induced autophagy and causes a severe, late-onset myopathy. *Cell metabolism*, 17(5), 731-744.
- Cervinková, Z., et al. (2007). Evaluation of mitochondrial function in isolated rat hepatocytes and mitochondria during oxidative stress. *Altern Lab Anim*, 35(3), 353-361. doi:10.1177/026119290703500303
- Chakravarty, E. F., Hubert, H. B., Lingala, V. B. and Fries, J. F. (2008). Reduced disability and mortality among aging runners: a 21-year longitudinal study. *Archives of internal medicine*, 168(15), 1638-1646.
- Chang, C.-Y., Liang, M.-Z. and Chen, L. (2019). Current progress of mitochondrial transplantation that promotes neuronal regeneration. *Translational neurodegeneration*, 8(1), 1-12.
- Chang, J.-C., et al. (2017). Peptide-mediated delivery of donor mitochondria improves mitochondrial function and cell viability in human cybrid cells with the MELAS A3243G mutation. *Scientific reports*, 7(1), 10710.
- Chen, L. K., et al. (2020). Asian Working Group for Sarcopenia: 2019 Consensus Update on Sarcopenia Diagnosis and Treatment. *J Am Med Dir Assoc*, 21(3), 300-307. e302. doi:10.1016/j.jamda.2019.12.012
- Chen, Y., Yang, F., Chu, Y., Yun, Z., Yan, Y. and Jin, J. (2022). Mitochondrial transplantation: opportunities and challenges in the treatment of obesity, diabetes, and nonalcoholic fatty liver disease. *Journal of Translational Medicine*, 20(1), 1-16.
- Cho, C.-H., Woo, J. S., Perez, C. F. and Lee, E. H. (2017). A focus on extracellular Ca²⁺ entry into skeletal muscle. *Experimental & molecular medicine*, 49(9), e378-e378.
- Cid-Díaz, T., et al. (2021). Obestatin signalling counteracts glucocorticoid-induced skeletal muscle atrophy via NEDD4/KLF15 axis. *Journal of Cachexia, Sarcopenia and Muscle*, 12(2), 493-505.
- Clark, M. A. and Shay, J. W. (1982). Mitochondrial transformation of mammalian cells. *Nature*, 295(5850), 605-607.
- Cohen, S., Zhai, B., Gygi, S. P. and Goldberg, A. L. (2012). Ubiquitylation by Trim32 causes coupled loss of desmin, Z-bands, and thin filaments in muscle atrophy. *J Cell Biol*, 198(4), 575-589. doi:10.1083/jcb.201110067
- Connolly, P., Garcia-Carpio, I. and Villunger, A. (2020). Cell-cycle cross talk with caspases and their substrates. *Cold Spring Harbor Perspectives in Biology*, 12(6), a036475.

- Cowan, D. B., *et al.* (2016). Intracoronary delivery of mitochondria to the ischemic heart for cardioprotection. *PLoS one*, *11*(8), e0160889.
- Crompton, M., Costi, A. and Hayat, L. (1987). Evidence for the presence of a reversible Ca²⁺-dependent pore activated by oxidative stress in heart mitochondria. *Biochemical journal*, *245*(3), 915-918.
- Danelson, K. A., *et al.* (2019). A military case review method to determine and record the mechanism of injury (BioTab) from in-theater attacks. *Military medicine*, *184*(Supplement_1), 374-378.
- Dave, H. D., Shook, M. and Varacallo, M. (2021). Anatomy, skeletal muscle *StatPearls [Internet]*: StatPearls Publishing.
- de Winter, J. M. and Ottenheijm, C. A. C. (2017). Sarcomere Dysfunction in Nemaline Myopathy. *J Neuromuscul Dis*, *4*(2), 99-113. doi:10.3233/jnd-160200
- Ekelund, U., *et al.* (2016). Does physical activity attenuate, or even eliminate, the detrimental association of sitting time with mortality? A harmonised meta-analysis of data from more than 1 million men and women. *The lancet*, *388*(10051), 1302-1310.
- Evans, W. J. (2010). Skeletal muscle loss: cachexia, sarcopenia, and inactivity. *The American journal of clinical nutrition*, *91*(4), 1123S-1127S.
- Fallaize, D., Chin, L.-S. and Li, L. (2015). Differential submitochondrial localization of PINK1 as a molecular switch for mediating distinct mitochondrial signaling pathways. *Cellular signalling*, *27*(12), 2543-2554.
- Farhana, A. and Lappin, S. L. (2020). Biochemistry, lactate dehydrogenase.
- Favaro, G., *et al.* (2019). DRP1-mediated mitochondrial shape controls calcium homeostasis and muscle mass. *Nature communications*, *10*(1), 2576.
- Finlay, L. D., Morris, A. C., Deane, A. M. and Wood, A. J. (2021). Neutrophil kinetics and function after major trauma: A systematic review. *World Journal of Critical Care Medicine*, *10*(5), 260.
- Flucher, B. E. and Tuluc, P. (2017). How and why are calcium currents curtailed in the skeletal muscle voltage-gated calcium channels? *The Journal of physiology*, *595*(5), 1451-1463.
- Fortin, M., Videman, T., Gibbons, L. E. and Battie, M. C. (2014). Paraspinal muscle morphology and composition: a 15-yr longitudinal magnetic resonance imaging study. *Medicine and science in sports and exercise*, *46*(5), 893-901.
- Friedrich, O., *et al.* (2015). The sick and the weak: neuropathies/myopathies in the critically ill. *Physiological reviews*, *95*(3), 1025-1109.
- Frontera, W. R. and Ochala, J. (2015). Skeletal muscle: a brief review of structure and function. *Calcified tissue international*, *96*, 183-195.
- Gäbelein, C. G., *et al.* (2022). Mitochondria transplantation between living cells. *PLoS Biology*, *20*(3), e3001576.
- Gao, Y., Waas, A. M., Faulkner, J. A., Kostrominova, T. Y. and Wineman, A. S. (2008). Micromechanical modeling of the epimysium of the skeletal muscles. *Journal of biomechanics*, *41*(1), 1-10.
- Gherardi, G., Di Marco, G., Rizzuto, R. and Mammucari, C. (2019). Crosstalk between mitochondrial Ca²⁺ uptake and autophagy in skeletal muscle. *Oxidative Medicine and Cellular Longevity*, 2019.
- Goll, D. E., Thompson, V. F., Li, H., Wei, W. and Cong, J. (2003). The calpain system. *Physiological reviews*.
- Gollihue, J. L., Patel, S. P. and Rabchevsky, A. G. (2018). Mitochondrial transplantation strategies as potential therapeutics for central nervous system trauma. *Neural Regen Res*, *13*(2), 194-197. doi:10.4103/1673-5374.226382

- Greising, S. M., Corona, B. T. and Call, J. A. (2020). Musculoskeletal regeneration, rehabilitation, and plasticity following traumatic injury. *International journal of sports medicine*, 41(08), 495-504.
- Greising, S. M., Dearth, C. L. and Corona, B. T. (2016). Regenerative and rehabilitative medicine: a necessary synergy for functional recovery from volumetric muscle loss injury. *Cells Tissues Organs*, 202(3-4), 237-249.
- Greising, S. M., et al. (2018). Early rehabilitation for volumetric muscle loss injury augments endogenous regenerative aspects of muscle strength and oxidative capacity. *BMC musculoskeletal disorders*, 19, 1-11.
- Grimm, P. D., Mauntel, T. C. and Potter, B. K. (2019). Combat and noncombat musculoskeletal injuries in the US military. *Sports medicine and arthroscopy review*, 27(3), 84-91.
- Grumati, P. and Bonaldo, P. (2012). Autophagy in Skeletal Muscle Homeostasis and in Muscular Dystrophies. *Cells*, 1(3), 325-345.
- Guo, J., Yin, Y., Jin, L., Zhang, R., Hou, Z. and Zhang, Y. (2019). Acute compartment syndrome: Cause, diagnosis, and new viewpoint. *Medicine*, 98(27).
- Haberecht-Müller, S., Krüger, E. and Fielitz, J. (2021). Out of Control: The Role of the Ubiquitin Proteasome System in Skeletal Muscle during Inflammation. *Biomolecules*, 11(9), 1327.
- Hah, Y.-S., et al. (2022). β -Sitosterol attenuates dexamethasone-induced muscle atrophy via regulating FoxO1-dependent signaling in C2C12 cell and mice model. *Nutrients*, 14(14), 2894.
- Hamel, Y., et al. (2021). Compromised mitochondrial quality control triggers lipin1-related rhabdomyolysis. *Cell Reports Medicine*, 2(8).
- Harris, J. (2003). Myotoxic phospholipases A2 and the regeneration of skeletal muscles. *Toxicon*, 42(8), 933-945.
- Hayashida, K., et al. (2023). Exogenous mitochondrial transplantation improves survival and neurological outcomes after resuscitation from cardiac arrest. *BMC medicine*, 21(1), 56.
- Hernández-Cruz, E. Y., Amador-Martínez, I., Aranda-Rivera, A. K., Cruz-Gregorio, A. and Chaverri, J. P. (2022). Renal damage induced by cadmium and its possible therapy by mitochondrial transplantation. *Chemico-Biological Interactions*, 361, 109961.
- Hodgens, A. and Sharman, T. (2022). Corticosteroids *StatPearls [Internet]*: StatPearls Publishing.
- Hopkins, P. M. (2006). Skeletal muscle physiology. *Continuing Education in Anaesthesia Critical Care & Pain*, 6(1), 1-6. doi:10.1093/bjaceaccp/mki062
- Hu, N.-F., et al. (2017). Tetramethylpyrazine ameliorated disuse-induced gastrocnemius muscle atrophy in hindlimb unloading rats through suppression of Ca²⁺/ROS-mediated apoptosis. *Applied Physiology, Nutrition, and Metabolism*, 42(2), 117-127.
- Huang, P.-J., et al. (2016). Transferring xenogenic mitochondria provides neural protection against ischemic stress in ischemic rat brains. *Cell transplantation*, 25(5), 913-927.
- Huang, Y., et al. (2019). Resveratrol prevents sarcopenic obesity by reversing mitochondrial dysfunction and oxidative stress via the PKA/LKB1/AMPK pathway. *Aging (Albany NY)*, 11(8), 2217.
- Huang, Z., et al. (2019). Skeletal muscle atrophy was alleviated by salidroside through suppressing oxidative stress and inflammation during denervation. *Frontiers in pharmacology*, 10, 997.

- Hung, V., *et al.* (2017). Proteomic mapping of cytosol-facing outer mitochondrial and ER membranes in living human cells by proximity biotinylation. *eLife*, 6, e24463. doi:10.7554/eLife.24463
- Irazoki, A., *et al.* (2023). Disruption of mitochondrial dynamics triggers muscle inflammation through interorganellar contacts and mitochondrial DNA mislocation. *Nature communications*, 14(1), 108.
- Irazoki, A., *et al.* (2022). Coordination of mitochondrial and lysosomal homeostasis mitigates inflammation and muscle atrophy during aging. *Aging Cell*, 21(4), e13583.
- Jennings, R. and Premanandan, C. (2017). *Veterinary histology*: Ohio State University.
- Jia, L., *et al.* (2022). Nrf2 participates in the protective effect of exogenous mitochondria against mitochondrial dysfunction in myocardial ischaemic and hypoxic injury. *Cellular signalling*, 92, 110266. doi:<https://doi.org/10.1016/j.cellsig.2022.110266>
- Jiaming, Y. and Rahimi, M. H. (2021). Creatine supplementation effect on recovery following exercise-induced muscle damage: A systematic review and meta-analysis of randomized controlled trials. *Journal of food biochemistry*, 45(10), e13916.
- Johnson, N. E. (2019). Myotonic Muscular Dystrophies. *Continuum (Minneapolis, Minn)*, 25(6), 1682-1695. doi:10.1212/con.0000000000000793
- Johnson, R. J., *et al.* (2007). Potential role of sugar (fructose) in the epidemic of hypertension, obesity and the metabolic syndrome, diabetes, kidney disease, and cardiovascular disease. *The American journal of clinical nutrition*, 86(4), 899-906.
- Jones, D. P. (2008). Radical-free biology of oxidative stress. *American Journal of Physiology-Cell Physiology*, 295(4), C849-C868.
- Jun, L., Robinson, M., Geetha, T., Broderick, T. L. and Babu, J. R. (2023). Prevalence and Mechanisms of Skeletal Muscle Atrophy in Metabolic Conditions. *International journal of molecular sciences*, 24(3), 2973.
- Jung, H.-W., Choi, J.-H., Jo, T., Shin, H. and Suh, J. M. (2019). Systemic and Local Phenotypes of Barium Chloride Induced Skeletal Muscle Injury in Mice. *Annals of geriatric medicine and research*, 23(2), 83.
- Jung, H. W., Choi, J. H., Jo, T., Shin, H. and Suh, J. M. (2019). Systemic and Local Phenotypes of Barium Chloride Induced Skeletal Muscle Injury in Mice. *Ann Geriatr Med Res*, 23(2), 83-89. doi:10.4235/agmr.19.0012
- Khodabukus, A. (2021). Tissue-engineered skeletal muscle models to study muscle function, plasticity, and disease. *Frontiers in Physiology*, 12, 619710.
- Kim, B., Kim, J.-S., Yoon, Y., Santiago, M. C., Brown, M. D. and Park, J.-Y. (2013). Inhibition of Drp1-dependent mitochondrial division impairs myogenic differentiation. *American Journal of Physiology-Regulatory, Integrative and Comparative Physiology*, 305(8), R927-R938.
- Kim, M. J., Lee, J. M., Min, K. and Choi, Y.-S. (2023). Xenogeneic transplantation of mitochondria induces muscle regeneration in an in vivo rat model of dexamethasone-induced atrophy. *Journal of Muscle Research and Cell Motility*, 1-16.
- King, M. P. and Attardi, G. (1988). Injection of mitochondria into human cells leads to a rapid replacement of the endogenous mitochondrial DNA. *Cell*, 52(6), 811-819.
- Knuth, C. M., Auger, C. and Jeschke, M. G. (2021). Burn-induced hypermetabolism and skeletal muscle dysfunction. *American Journal of Physiology-Cell Physiology*, 321(7), C58-C71.

- Ku, S.-K., Lim, J.-M., Cho, H.-R., Bashir, K. M. I., Kim, Y. S. and Choi, J.-S. (2021). Tart Cherry (Fruit of *Prunus cerasus*) Concentrated Powder (TCcp) Ameliorates Glucocorticoid-Induced Muscular Atrophy in Mice. *Medicina*, 57(5), 485.
- Kubat, G. B., *et al.* (2021). The effects of mesenchymal stem cell mitochondrial transplantation on doxorubicin-mediated nephrotoxicity in rats. *Journal of biochemical and molecular toxicology*, 35(1), e22612.
- Kunz, H. E., *et al.* (2020). Methylarginine metabolites are associated with attenuated muscle protein synthesis in cancer-associated muscle wasting. *J Biol Chem*, 295(51), 17441-17459. doi:10.1074/jbc.RA120.014884
- Kuo, I. Y. and Ehrlich, B. E. (2015). Signaling in muscle contraction. *Cold Spring Harbor Perspect Biol*, 7(2), a006023. doi:10.1101/cshperspect.a006023
- Kurrat, A., *et al.* (2015). Lifelong exposure to dietary isoflavones reduces risk of obesity in ovariectomized Wistar rats. *Mol Nutr Food Res*, 59(12), 2407-2418. doi:10.1002/mnfr.201500240
- Lang, C., Sittl, H. and Erbguth, F. (1997). Coenzyme Q10 Treatment in Mitochondrial Encephalomyopathies. *European Neurology*, 37(4), 212-218.
- Langone, F., *et al.* (2014). Metformin protects skeletal muscle from cardiotoxin induced degeneration. *PLoS one*, 9(12), e114018.
- Lavender, A. P. and Nosaka, K. (2006). Changes in fluctuation of isometric force following eccentric and concentric exercise of the elbow flexors. *European journal of applied physiology*, 96, 235-240.
- Lecker, S. H., *et al.* (2004). Multiple types of skeletal muscle atrophy involve a common program of changes in gene expression. *Faseb j*, 18(1), 39-51. doi:10.1096/fj.03-0610com
- Lejay, A., *et al.* (2018). N-Acetyl cysteine restores limb function, improves mitochondrial respiration, and reduces oxidative stress in a murine model of critical limb ischaemia. *European Journal of Vascular and Endovascular Surgery*, 56(5), 730-738.
- Lerman-Sagie, T., *et al.* (2001). Dramatic improvement in mitochondrial cardiomyopathy following treatment with idebenone. *Journal of inherited metabolic disease*, 24, 28-34.
- Liang, J.-L., Xie, J.-F., Wang, C.-Y. and Chen, N. (2020a). Regulatory roles of microRNAs in sarcopenia and exercise intervention. *Sheng li xue bao: [Acta Physiologica Sinica]*, 72(5), 667-676.
- Liang, J.-L., Xie, J.-F., Wang, C.-Y. and Chen, N. (2020b). [Regulatory roles of microRNAs in sarcopenia and exercise intervention]. *Sheng li xue bao: [Acta Physiologica Sinica]*, 72(5), 667-676.
- Liao, P., Zhou, J., Ji, L. L. and Zhang, Y. (2010). Eccentric contraction induces inflammatory responses in rat skeletal muscle: role of tumor necrosis factor- α . *American Journal of Physiology-Regulatory, Integrative and Comparative Physiology*, 298(3), R599-R607.
- Liet, J.-M., *et al.* (2003). The effect of short-term dimethylglycine treatment on oxygen consumption in cytochrome oxidase deficiency: a double-blind randomized crossover clinical trial. *The Journal of pediatrics*, 142(1), 62-66.
- Lim, J.-M., *et al.* (2019). Protective effects of triple fermented barley extract (FBe) on indomethacin-induced gastric mucosal damage in rats. *BMC Complementary and Alternative medicine*, 19, 1-11.
- Lim, J. M., *et al.* (2018). Extracellular polysaccharides purified from *Aureobasidium pullulans* SM-2001 (Polycan) inhibit dexamethasone-induced muscle atrophy in mice. *International Journal of Molecular Medicine*, 41(3), 1245-1264.
- Lin, H.-C., Liu, S.-Y., Lai, H.-S. and Lai, I.-R. (2013). Isolated mitochondria infusion mitigates ischemia-reperfusion injury of the liver in rats. *Shock*, 39(3), 304-310.

- Liu, C., *et al.* (2019). Enhanced autophagy alleviates injury during hindlimb ischemia/reperfusion in mice. *Experimental and Therapeutic Medicine*, 18(3), 1669-1676.
- Liu, J. C., *et al.* (2020). EMRE is essential for mitochondrial calcium uniporter activity in a mouse model. *JCI insight*, 5(4).
- Liu, Z., Sun, Y., Qi, Z., Cao, L. and Ding, S. (2022). Mitochondrial transfer/transplantation: An emerging therapeutic approach for multiple diseases. *Cell & Bioscience*, 12(1), 1-29.
- Mahdy, M. A. A. (2019). Biotoxins in muscle regeneration research. *Journal of Muscle Research and Cell Motility*, 40(3), 291-297. doi:10.1007/s10974-019-09548-4
- Mansour, Z., *et al.* (2012). Remote and local ischemic preconditioning equivalently protects rat skeletal muscle mitochondrial function during experimental aortic cross-clamping. *Journal of vascular surgery*, 55(2), 497-505. e491.
- Maqoud, F., Cetrone, M., Mele, A. and Tricarico, D. (2017). Molecular structure and function of big calcium-activated potassium channels in skeletal muscle: pharmacological perspectives. *Physiological genomics*, 49(6), 306-317.
- Masiero, E., *et al.* (2009). Autophagy is required to maintain muscle mass. *Cell metabolism*, 10(6), 507-515.
- Masuzawa, A., *et al.* (2013). Transplantation of autologously derived mitochondria protects the heart from ischemia-reperfusion injury. *American Journal of Physiology-Heart and Circulatory Physiology*, 304(7), H966-H982.
- McCuller, C., Jessu, R. and Callahan, A. L. (2022). Physiology, skeletal muscle *StatPearls [Internet]*: StatPearls Publishing.
- McCully, J. D., Cowan, D. B., Pacak, C. A., Toumpoulis, I. K., Dayalan, H. and Levitsky, S. (2009). Injection of isolated mitochondria during early reperfusion for cardioprotection. *American Journal of Physiology-Heart and Circulatory Physiology*, 296(1), H94-H105.
- McGrath, M. J., *et al.* (2021). Defective lysosome reformation during autophagy causes skeletal muscle disease. *The Journal of clinical investigation*, 131(1).
- Memme, J. M., Erlich, A. T., Phukan, G. and Hood, D. A. (2021). Exercise and mitochondrial health. *The Journal of physiology*, 599(3), 803-817.
- Meng, Q., *et al.* (2020). Flavonoids extracted from mulberry (*Morus alba* L.) leaf improve skeletal muscle mitochondrial function by activating AMPK in type 2 diabetes. *Journal of Ethnopharmacology*, 248, 112326.
- Michelucci, A., Liang, C., Protasi, F. and Dirksen, R. T. (2021). Altered Ca²⁺ Handling and Oxidative Stress Underlie Mitochondrial Damage and Skeletal Muscle Dysfunction in Aging and Disease. *Metabolites*, 11(7), 424.
- Moreira, J. B. N., Wohlwend, M. and Wisløff, U. (2020). Exercise and cardiac health: physiological and molecular insights. *Nat Metab*, 2(9), 829-839. doi:10.1038/s42255-020-0262-1
- Morris, J. L., Gillet, G., Prudent, J. and Popgeorgiev, N. (2021). Bcl-2 family of proteins in the control of mitochondrial calcium signalling: an old chap with new roles. *International journal of molecular sciences*, 22(7), 3730.
- Morton, A. B., Norton, C. E., Jacobsen, N. L., Fernando, C. A., Cornelison, D. and Segal, S. S. (2019). Barium chloride injures myofibers through calcium-induced proteolysis with fragmentation of motor nerves and microvessels. *Skeletal muscle*, 9(1), 1-10.
- Morton, A. B., Norton, C. E., Jacobsen, N. L., Fernando, C. A., Cornelison, D. D. W. and Segal, S. S. (2019). Barium chloride injures myofibers through calcium-induced proteolysis with fragmentation of motor nerves and microvessels. *Skeletal Muscle*, 9(1), 27. doi:10.1186/s13395-019-0213-2

- Mukund, K. and Subramaniam, S. (2020). Skeletal muscle: A review of molecular structure and function, in health and disease. *Wiley Interdisciplinary Reviews: Systems Biology and Medicine*, 12(1), e1462.
- Munkanatta Godage, D. N., et al. (2018). SMYD2 glutathionylation contributes to degradation of sarcomeric proteins. *Nature communications*, 9(1), 4341.
- Murgia, M., Nogara, L., Baraldo, M., Reggiani, C., Mann, M. and Schiaffino, S. (2021). Protein profile of fiber types in human skeletal muscle: a single-fiber proteomics study. *Skeletal muscle*, 11(1), 1-19.
- Murphy, M. P. (2009). How mitochondria produce reactive oxygen species. *Biochemical journal*, 417(1), 1-13.
- Murphy, M. P. and Smith, R. A. (2000). Drug delivery to mitochondria: the key to mitochondrial medicine. *Advanced drug delivery reviews*, 41(2), 235-250.
- Nazio, F., et al. (2013). mTOR inhibits autophagy by controlling ULK1 ubiquitylation, self-association and function through AMBRA1 and TRAF6. *Nat Cell Biol*, 15(4), 406-416. doi:10.1038/ncb2708
- Oba, K., et al. (2020). Serum growth differentiation factor 15 level is associated with muscle strength and lower extremity function in older patients with cardiometabolic disease. *Geriatrics & Gerontology International*, 20(10), 980-987.
- Ono, Y., Saido, T. C. and Sorimachi, H. (2016). Calpain research for drug discovery: challenges and potential. *Nature Reviews Drug Discovery*, 15(12), 854-876.
- Orfany, A., et al. (2020). Mitochondrial transplantation ameliorates acute limb ischemia. *Journal of vascular surgery*, 71(3), 1014-1026.
- Ozaki, Y., et al. (2023). Myonectin protects against skeletal muscle dysfunction in male mice through activation of AMPK/PGC1 α pathway. *Nature communications*, 14(1), 4675.
- Paez, H. G., Pitzer, C. R. and Alway, S. E. (2023). Age-related dysfunction in proteostasis and cellular quality control in the development of sarcopenia. *Cells*, 12(2), 249.
- Park, A., et al. (2021). Mitochondrial transplantation as a novel therapeutic strategy for mitochondrial diseases. *International journal of molecular sciences*, 22(9), 4793.
- Paul, P. K., et al. (2010). Targeted ablation of TRAF6 inhibits skeletal muscle wasting in mice. *J Cell Biol*, 191(7), 1395-1411. doi:10.1083/jcb.201006098
- Pellegrino, M., Canepari, M., Rossi, R., D'antona, G., Reggiani, C. and Bottinelli, R. (2003). Orthologous myosin isoforms and scaling of shortening velocity with body size in mouse, rat, rabbit and human muscles. *The Journal of Physiology*, 546(3), 677-689.
- Peruzzotti-Jametti, L., et al. (2021). Neural stem cells traffic functional mitochondria via extracellular vesicles. *PLoS Biology*, 19(4), e3001166.
- Pham, S. and Puckett, Y. (2020). Physiology, Skeletal Muscle Contraction.
- Phung, L. A., Foster, A. D., Miller, M. S., Lowe, D. A. and Thomas, D. D. (2020). Super-relaxed state of myosin in human skeletal muscle is fiber-type dependent. *American Journal of Physiology-Cell Physiology*, 319(6), C1158-C1162.
- Porter, C., et al. (2016). Long-term skeletal muscle mitochondrial dysfunction is associated with hypermetabolism in severely burned children. *Journal of Burn Care & Research*, 37(1), 53-63.
- Pranoto, A., et al. (2023). Long-Term Resistance-Endurance Combined Training Reduces Pro-Inflammatory Cytokines in Young Adult Females with Obesity. *Sports (Basel)*, 11(3). doi:10.3390/sports11030054

- Qin, J., *et al.* (2013). Dexamethasone-induced skeletal muscle atrophy was associated with upregulation of myostatin promoter activity. *Research in veterinary science*, 94(1), 84-89.
- Quinlan, C. L., Perevoshchikova, I. V., Hey-Mogensen, M., Orr, A. L. and Brand, M. D. (2013). Sites of reactive oxygen species generation by mitochondria oxidizing different substrates. *Redox biology*, 1(1), 304-312.
- Rahman, F. A. and Quadriatero, J. (2021). Mitochondrial network remodeling: An important feature of myogenesis and skeletal muscle regeneration. *Cellular and Molecular Life Sciences*, 78, 4653-4675.
- Raven, P. B., Wasserman, D. H., Squires, W. G. and Murray, T. D. (2012). *Exercise Physiology*: Cengage Learning.
- Rivera, J. C. and Corona, B. T. (2016). Muscle-related Disability Following Combat Injury Increases With Time. *US Army Medical Department journal*.
- Robichaux, D. J., Harata, M., Murphy, E. and Karch, J. (2022). Mitochondrial permeability transition pore-dependent necrosis. *Journal of molecular and cellular cardiology*.
- Rodney, G. G., Pal, R. and Abo-Zahrah, R. (2016). Redox regulation of autophagy in skeletal muscle. *Free Radical Biology and Medicine*, 98, 103-112.
- Rome, L. C., *et al.* (1988). Why animals have different muscle fibre types. *Nature*, 335, 824-827.
- Roshanravan, B., *et al.* (2021). In vivo mitochondrial ATP production is improved in older adult skeletal muscle after a single dose of elamipretide in a randomized trial. *PloS one*, 16(7), e0253849.
- Salucci, S. and Falcieri, E. (2020). Polyphenols and their potential role in preventing skeletal muscle atrophy. *Nutrition Research*, 74, 10-22.
- Sandri, M., *et al.* (2013). Signalling pathways regulating muscle mass in ageing skeletal muscle: the role of the IGF1-Akt-mTOR-FoxO pathway. *Biogerontology*, 14(3), 303-323. doi:10.1007/s10522-013-9432-9
- Sarraf, S. A., *et al.* (2013). Landscape of the PARKIN-dependent ubiquitylome in response to mitochondrial depolarization. *Nature*, 496(7445), 372-376.
- Sartori, R., Romanello, V. and Sandri, M. (2021). Mechanisms of muscle atrophy and hypertrophy: implications in health and disease. *Nat Commun*, 12(1), 330. doi:10.1038/s41467-020-20123-1
- Sartori, R., Romanello, V. and Sandri, M. (2021). Mechanisms of muscle atrophy and hypertrophy: Implications in health and disease. *Nature communications*, 12(1), 330.
- Sartori, R., *et al.* (2013). BMP signaling controls muscle mass. *Nat Genet*, 45(11), 1309-1318. doi:10.1038/ng.2772
- Schiaffino, S., Dyar, K. A., Ciciliot, S., Blaauw, B. and Sandri, M. (2013). Mechanisms regulating skeletal muscle growth and atrophy. *The FEBS Journal*, 280(17), 4294-4314. doi:<https://doi.org/10.1111/febs.12253>
- Schiaffino, S. and Reggiani, C. (2011). Fiber types in mammalian skeletal muscles. *Physiological reviews*, 91(4), 1447-1531.
- Schoenfeld, B. J. (2010). The mechanisms of muscle hypertrophy and their application to resistance training. *J Strength Cond Res*, 24(10), 2857-2872. doi:10.1519/JSC.0b013e3181e840f3
- Seidlmayer, L. K., Juettner, V. V., Kettlewell, S., Pavlov, E. V., Blatter, L. A. and Dedkova, E. N. (2015). Distinct mPTP activation mechanisms in ischaemia-reperfusion: contributions of Ca²⁺, ROS, pH, and inorganic polyphosphate. *Cardiovascular research*, 106(2), 237-248.

- Seo, E., Truong, C.-S. and Jun, H.-S. (2022). Psoralea corylifolia L. seed extract attenuates dexamethasone-induced muscle atrophy in mice by inhibition of oxidative stress and inflammation. *Journal of Ethnopharmacology*, 296, 115490.
- Sercel, A. J., et al. (2021). Stable transplantation of human mitochondrial DNA by high-throughput, pressurized isolated mitochondrial delivery. *eLife*, 10, e63102.
- Sewright, K. A., Hubal, M. J., Kearns, A., Holbrook, M. T. and Clarkson, P. M. (2008). Sex differences in response to maximal eccentric exercise. *Medicine and science in sports and exercise*, 40(2), 242-251.
- Silva, K. A. S., et al. (2015). Inhibition of Stat3 activation suppresses caspase-3 and the ubiquitin-proteasome system, leading to preservation of muscle mass in cancer cachexia. *Journal of Biological Chemistry*, 290(17), 11177-11187.
- Slavin, M. B., Memme, J. M., Oliveira, A. N., Moradi, N. and Hood, D. A. (2022). Regulatory networks coordinating mitochondrial quality control in skeletal muscle. *American Journal of Physiology-Cell Physiology*, 322(5), C913-C926.
- Sliter, D. A., et al. (2018). Parkin and PINK1 mitigate STING-induced inflammation. *Nature*, 561(7722), 258-262.
- Smith, J. A., Murach, K. A., Dyar, K. A. and Zierath, J. R. (2023). Exercise metabolism and adaptation in skeletal muscle. *Nature Reviews Molecular Cell Biology*, 1-26.
- Smith, J. K., Carden, D. L. and Korthuis, R. J. (1989). Role of xanthine oxidase in postischemic microvascular injury in skeletal muscle. *Am J Physiol*, 257(6 Pt 2), H1782-1789. doi:10.1152/ajpheart.1989.257.6.H1782
- Sorimachi, H., Hata, S. and Ono, Y. (2011). Calpain chronicle—an enzyme family under multidisciplinary characterization. *Proceedings of the Japan Academy, Series B*, 87(6), 287-327.
- Sousa-Victor, P. and Muñoz-Cánoves, P. (2016). Regenerative decline of stem cells in sarcopenia. *Molecular aspects of medicine*, 50, 109-117.
- Southern, W. M., et al. (2019). PGC-1 α overexpression partially rescues impaired oxidative and contractile pathophysiology following volumetric muscle loss injury. *Scientific reports*, 9(1), 4079.
- Straight, C. R., Fedewa, M. V., Toth, M. J. and Miller, M. S. (2020). Improvements in skeletal muscle fiber size with resistance training are age-dependent in older adults: a systematic review and meta-analysis. *Journal of applied physiology*, 129(2), 392-403.
- Tezze, C., et al. (2017). Age-associated loss of OPA1 in muscle impacts muscle mass, metabolic homeostasis, systemic inflammation, and epithelial senescence. *Cell metabolism*, 25(6), 1374-1389. e1376.
- Tieland, M., Trouwborst, I. and Clark, B. C. (2018). Skeletal muscle performance and ageing. *Journal of Cachexia, Sarcopenia and Muscle*, 9(1), 3-19.
- Torigoe, K., Tanaka, H.-F., Takahashi, A., Awaya, A. and Hashimoto, K. (1996). Basic behavior of migratory Schwann cells in peripheral nerve regeneration. *Experimental neurology*, 137(2), 301-308.
- Torres, P. A., Helmstetter, J. A., Kaye, A. M. and Kaye, A. D. (2015). Rhabdomyolysis: pathogenesis, diagnosis, and treatment. *Ochsner J*, 15(1), 58-69.
- Tria, F. D., et al. (2021). Gene duplications trace mitochondria to the onset of eukaryote complexity. *Genome biology and evolution*, 13(5), evab055.
- Turner, P. R., Westwood, T., Regen, C. M. and Steinhardt, R. A. (1988). Increased protein degradation results from elevated free calcium levels found in muscle from mdx mice. *Nature*, 335(6192), 735-738.
- Ulger, O. and Kubat, G. B. (2022). Therapeutic applications of mitochondrial transplantation. *Biochimie*, 195, 1-15.
doi:<https://doi.org/10.1016/j.biochi.2022.01.002>

- Vainshtein, A. and Sandri, M. (2020). Signaling Pathways That Control Muscle Mass. *Int J Mol Sci*, 21(13). doi:10.3390/ijms21134759
- Wagatsuma, A., Kotake, N. and Yamada, S. (2011). Muscle regeneration occurs to coincide with mitochondrial biogenesis. *Molecular and cellular biochemistry*, 349, 139-147.
- Wallace, D. C., Fan, W. and Procaccio, V. (2010). Mitochondrial energetics and therapeutics. *Annual Review of Pathology: Mechanisms of Disease*, 5, 297-348.
- Wang, B. Y.-H., et al. (2023). Mesenchymal stem cells alleviate dexamethasone-induced muscle atrophy in mice and the involvement of ERK1/2 signalling pathway. *Stem Cell Research & Therapy*, 14(1), 195.
- Wang, X., et al. (2013). Transient systemic mtDNA damage leads to muscle wasting by reducing the satellite cell pool. *Human molecular genetics*, 22(19), 3976-3986.
- Wang, Y., et al. (2019). Mitochondrial transplantation attenuates lipopolysaccharide-induced depression-like behaviors. *Progress in Neuro-Psychopharmacology and Biological Psychiatry*, 93, 240-249.
doi:<https://doi.org/10.1016/j.pnpbp.2019.04.010>
- Wu, N. N., Tian, H., Chen, P., Wang, D., Ren, J. and Zhang, Y. (2019). Physical Exercise and Selective Autophagy: Benefit and Risk on Cardiovascular Health. *Cells*, 8(11). doi:10.3390/cells8111436
- Wu, Y.-C., et al. (2015). Massively parallel delivery of large cargo into mammalian cells with light pulses. *Nature methods*, 12(5), 439-444.
- Xie, Q., et al. (2021). Mitochondrial transplantation attenuates cerebral ischemia-reperfusion injury: possible involvement of mitochondrial component separation. *Oxidative Medicine and Cellular Longevity*, 2021.
- Yamada, Y., Ito, M., Arai, M., Hibino, M., Tsujioka, T. and Harashima, H. (2020). Challenges in promoting mitochondrial transplantation therapy. *International journal of molecular sciences*, 21(17), 6365.
- Yin, L., et al. (2021). Skeletal muscle atrophy: From mechanisms to treatments. *Pharmacol Res*, 172, 105807. doi:10.1016/j.phrs.2021.105807
- Yin, L., et al. (2021). Skeletal muscle atrophy: From mechanisms to treatments. *Pharmacological research*, 172, 105807.
- Yoshikawa, M., Hosokawa, M., Miyashita, K., Nishino, H. and Hashimoto, T. (2021). Effects of fucoxanthin on the inhibition of dexamethasone-induced skeletal muscle loss in mice. *Nutrients*, 13(4), 1079.
- Zhelankin, A. V., Iulmetova, L. N., Ahmetov, I. I., Generozov, E. V. and Sharova, E. I. (2023). Diversity and Differential Expression of MicroRNAs in the Human Skeletal Muscle with Distinct Fiber Type Composition. *Life*, 13(3), 659.
- Zhou, J., Liu, B., Liang, C., Li, Y. and Song, Y.-H. (2016). Cytokine signaling in skeletal muscle wasting. *Trends in Endocrinology & Metabolism*, 27(5), 335-347.
- Zorov, D. B., Filburn, C. R., Klotz, L.-O., Zweier, J. L. and Sollott, S. J. (2000). Reactive oxygen species (Ros-Induced) Ros release: A new phenomenon accompanying induction of the mitochondrial permeability transition in cardiac myocytes. *The Journal of experimental medicine*, 192(7), 1001-1014.
- Zumbaugh, M. D., Johnson, S. E., Shi, T. H. and Gerrard, D. E. (2022). Molecular and biochemical regulation of skeletal muscle metabolism. *J Anim Sci*, 100(8). doi:10.1093/jas/skac035
- Zumbaugh, M. D., Johnson, S. E., Shi, T. H. and Gerrard, D. E. (2022). Molecular and biochemical regulation of skeletal muscle metabolism. *Journal of Animal Science*, 100(8), skac035.

The Impact of Exogenous Mitochondrial Transfer on Skeletal Muscle Injuries in Mice

ORIGINALITY REPORT

| | | | |
|------------------|------------------|--------------|----------------|
| 5 % | 4 % | 4 % | % |
| SIMILARITY INDEX | INTERNET SOURCES | PUBLICATIONS | STUDENT PAPERS |

PRIMARY SOURCES

| | | |
|----------|---|----------------|
| 1 | Marco D'Amato, Francesca Morra, Ivano Di Di Meo, Valeria Tiranti. "Mitochondrial Transplantation in Mitochondrial Medicine: Current Challenges and Future Perspectives", International Journal of Molecular Sciences, 2023 Publication | 1 % |
| 2 | www.powershow.com Internet Source | 1 % |
| 3 | theses.gla.ac.uk Internet Source | <1 % |
| 4 | d-nb.info Internet Source | <1 % |
| 5 | estudogeral.sib.uc.pt Internet Source | <1 % |
| 6 | pr.hec.gov.pk Internet Source | <1 % |
| 7 | www.mdpi.com Internet Source | <1 % |